Review Article

Nano Research
2022, 15(7): 6220–6242

ISSN 1998-0124 CN 11-5974/O4
https://doi.org/10.1007/s12274-022-4302-x

Recent advances in metal-organic framework-based materials for anti-staphylococcus aureus infection

Mei Yang[1], Jin Zhang[2], Yinhao Wei[1], Jie Zhang[2] (✉), and Chuanmin Tao[1] (✉)

[1] *Department of Laboratory Medicine, West China Hospital, Sichuan University, Chengdu 610041, China*
[2] *College of Materials Science and Engineering, Sichuan University, Chengdu 610065, China*

© Tsinghua University Press 2022

Received: 14 January 2022 / **Revised:** 4 March 2022 / **Accepted:** 7 March 2022

ABSTRACT

The rapid spread of *staphylococcus aureus* (*S. aureus*) causes an increased morbidity and mortality, as well as great economic losses in the world. Anti-*S. aureus* infection becomes a major challenge for clinicians and nursing professionals to address drug resistance. Hence, it is urgent to explore high efficiency, low toxicity, and environmental-friendly methods against *S. aureus*. Metal-organic frameworks (MOFs) represent great potential in treating *S. aureus* infection due to the unique features of MOFs including tunable chemical constitute, open crystalline structure, and high specific surface area. Especially, these properties endow MOF-based materials outstanding antibacterial effect, which can be mainly attributed to the continuously released active components and the exerted catalytic activity to fight bacterial infection. Herein, the structural characteristics of MOFs and evaluation method of antimicrobial activity are briefly summarized. Then we systematically give an overview on their recent progress on antibacterial mechanisms, metal ion sustained-release system, controlled delivery system, catalytic system, and energy conversion system based on MOF materials. Finally, suggestions and direction for future research to develop and mechanism understand MOF-based materials are discussed in antibacterial application.

KEYWORDS

staphylococcus aureus (*S. aureus*), metal-organic frameworks, antimicrobial activity, antibacterial mechanisms, controlled drug delivery systems

1 Introduction

Staphylococcus aureus (*S. aureus*) belongs to a Gram-positive bacterium with grape-like clusters (approximately 0.8 μm in diameter) and regarded as the human commensal of the Micrococcaceae family. *S. aureus* is a frequent colonizer that often presents on various parts of body such as oral cavity, perineum, axilla, mucous membranes [1], anterior nares [2], and guts of healthy individuals. Colonization is the major risk factor for the development of clinical *S. aureus* infection, including the colonization types of non-carriage, intermittent colonization, and persistent colonization [3, 4]. Moreover, *S. aureus* also is vital human pathogen that causes a series of infections on skin, wounds, soft tissues, arthroses, bones, and the associated infections in indwelling catheters or prosthesis [5]. Simultaneously, it is a leading cause of sepsis and infective endocarditis (IE) infections [6]. Besides, *S. aureus* is also a common pathogen of biofilms and often associated with infections of implanted medical materials, such as catheters and artificial heart valves. The rapid spread of *S. aureus* has resulted in an increased morbidity and mortality, as well as great economic losses in the world [7].

Although the discovery of antibiotics have displayed positive effects in treating *S. aureus* infections, the abuse and misapplication of antibiotics increase the selection pressure for resistant strains and decrease the effectiveness of antibiotics [8]. It further produces larger quantities of robust strains with multidrug-resistant (MDR) [9], such as the typical methicillin-resistant *S. aureus* (MRSA). In addition, *S. aureus* coalesced into a biofilm in stressful environments, which can protect active cells from the effects of antibacterial agents and host defense mechanisms. Thus, the infections caused by *S. aureus* bring about a series of severe health problems, but the available therapeutics is limited at the current stage.

To date, numerous efforts have been made to explore novel antimicrobial materials for treatment of bacterial infections, such as metal compounds, cationic polymers, nano-enzymes, and metal-organic frameworks (MOFs). Among these wide categories of promising antimicrobial nanomaterials, MOFs are considered as a classical porous coordination polymer self-assembled by metal ions and organic ligands, developing as featured nanoplatform for biomedical applications [10, 11]. MOFs exhibit tunable chemical constitute, open crystalline structure with large surface area, controllable pore structures and internal/external surface [12], which also endow it a broad application prospect in gas adsorption [13], catalysis [11], biological imaging, and energy storage/conversion [14]. In addition, MOFs also have been well developed in the antibacterial field in the past decade and are still fast growing, with thousands of researchers reported each year.

Previous reviews mainly focused on the characteristics, structure, antibacterial mechanism, and application of MOF-based nanomaterials [12, 15, 18]. Furthermore, *S. aureus* colonization, transmission mode, clinical hazards, and pathogenicity are rarely mentioned, especially the harm of drug-resistant MRSA. In this

Address correspondence to Jie Zhang, jzhangchem@scu.edu.cn; Chuanmin Tao, taocm@scu.edu.cn

review, we emphasize the importance of antimicrobial strategies based on MOF-based nanomaterials aiming at *S. aureus* and MRSA. In particular, evaluation of antibacterial activity is summarized according to the experience and practice from our research group, laboratory and hospital. Specially, the diversified antibacterial mechanisms of MOF-based nanomaterials against *S. aureus*, such as metal ion sustained release system, catalytic system, drug delivery system, and energy excitation system are introduced in detail. Besides this, we also highlight the relationship between the MOF-based nanomaterials and antibacterial effect, and discuss the construction of materials that can be used to extend the medical application in vivo and implantation. Finally, challenges as well as prospects are critically discussed for the future development of MOFs. Through the discussions, we expect to illustrate some points on the exploration of MOFs-based materials for promising application.

2 *S. aureus*

2.1 *S. aureus* colonization

S. aureus often causes a wide range of infections as crucial pathogens [17], with up to 20%–30% of persistently asymptomatic colonization and 50%–60% of intermittent colonization [18, 19]. For example, both methicillin-sensitive and methicillin-resistant strains isolates are persistent colonizers. *S. aureus* colonization frequently occurs among patients with diabetes, surgical patients, drug injectors, and immunocompromised patients [20, 21]. Processes of *S. aureus* infection include colonization, local infection, systematic dissemination, metastatic infection, and toxicosis [22]. Given the above situations, *S. aureus* colonization has been considered as a risk factor to resulting in the subsequent infections.

2.2 Mode of transmission

Hand hygiene plays an important role in the transmission associated with *S. aureus* infections and is the primary measure to prevent cross-infection in hospitals [23]. The hands of health care workers can be temporarily colonized by *S. aureus* through contact with their own or bacterial storage pools of the infected patients. Long-term exposure to *S. aureus* carrier or bacterial storage pools can cause a serious bacterial transmission and infection outbreak [24]. In addition, water, food, air, contact, biological vectors, and iatrogenic infections also could bring about the large-scale spread of *S. aureus*.

2.3 Clinical hazards and pathogenicity

The diseases caused by *S. aureus* infections can be divided into common and uncommon diseases, ranging from slight skin infection to the life-threatening diseases. The common diseases associated with *S. aureus* include sepsis, infective endocarditis, osteoarditis, pleurisy, skin infection, and food poisoning. Uncommon diseases involve meningitis, epifolliculitis, mastitis, urinary tract infection, endocarditis, biofilm-associated infection [5], etc. In particular, *S. aureus* and its biofilms can also cause a series of implant-related infections. The possible mechanism is that implants (such as prosthetic devices and electronic devices) act as a surface for *S. aureus* or biofilms to colonize. By avoiding the killing effects of phagocytes and increasing antibiotic resistance, the bacteria cause incurable infected tissue [25]. *S. aureus* can produce golden pigment, plasma coagulase positive, decompose mannitol, exhibiting strong pathogenicity. In addition, the strong infection ability of *S. aureus* can be ascribed to the produced various resistance mechanisms and virulence factors. The involved toxins, exotoxins, enzymes, and cell surface-associated antigens allow *S. aureus* could evade host natural defenses [26, 27]. In general, multifunctional toxins coordinated with their multiple enzymatic activities could degrade some host cells, decrease immune responses, and even manipulate the innate and adaptative immune responses. The above consequences promote the reproduction and spread of *S. aureus* [28]. When *S. aureus* invades the body, the enzyme causes fibrin depositing in blood, plasma, or coagulum on surface of the bacterium, blocking the phagocytosis of phagocytes [29]. Therefore, the clinical hazards and pathogenicity of *S. aureus* cannot be ignored in research field of antimicrobial materials.

2.4 Status of MDR

Although remarkable efforts have been dedicated to developing novel antimicrobial materials with high efficiency [30, 31], it inevitably raised the number of MDR bacteria [32, 33]. The main reason for the continuous occurrence of MDR lies in the abuse and misuse of antibiotics, which makes them insensitive to most antibiotics in current clinical application and generates more robust strains with MDR [34, 35]. The previous reports indicated that MRSA strains show increased resistance to all β-lactam antibiotics including penicillin and cephalosporins (except ceftaroline and ceftobiprole), accounting for at least 25%–50% of *S. aureus* infections in hospitals [36].

The Centers for Disease Control and Prevention reported about 80,000 serious MRSA infections happened in the United States during 2011, with 11,000 deaths each year [37]. In 2012, MRSA was estimated to have infected more than 75,000 patients, resulting in more than 9,600 deaths in the USA [38]. In addition, more than half of hospitals in most Asian countries got infections caused by MRSA [39]. More seriously, MRSA infections resulted in an increased burden on health care, which is ascribed to the increased hospital stays, health care costs, and the reduced life quality [40–42]. Thus, the increased MRSA resistance is deemed as a serious health problem of against the conventional medical antimicrobial agents. To ameliorate this dilemma, many new antimicrobial strategies have been carried out by researchers to develop the novel therapies for infections caused by MDR organisms [43].

2.5 Biofilm formed by *S. aureus*

Bacterial biofilm refers to a large number of bacterial aggregation membranes, formed by bacteria adhering to the contact surface, secreting polysaccharide matrix, fibrin, lipid protein, and wrapping themselves [44]. Once the biofilm formed, it has natural resistance to antibiotics and body immunity. Antibiotics cannot effectively remove the biofilm, and bacterial resistance will continue to grow in various ways [45–47]. Especially, *S. aureus* presents a variety of mechanisms for adhesion to host tissues and bodies. Once adhered, microcolonies can be formed and then reproduced through generating extracellular matrix to form biofilms. More seriously, *S. aureus* can not only form biofilms on different surfaces and medical instruments (such as surgical instruments and implants) in medical institutions, but also produce biofilms in infected host tissues, which may cause surgical risks [48]. Therefore, new therapeutic strategies are urgently needed to address *S. aureus* biofilm-associated infections.

3 Structure and characteristics of MOFs

MOFs are becoming as a wide category of greatly emerging porous materials via coordination bond connections between metal nodes and organic linkers [49, 50]. Different from conventional porous materials, MOFs have the advantages of three-dimensional (3D) pore structure, high porosity, large surface

area, strong regulation of skeleton structure, easy to modification, and unique photoelectric properties [51]. Moreover, their structure and physicochemical properties can be adjusted by rational design and tailor through "post-synthesis" and other functional modifications [52]. More importantly, the various topological structures of MOFs can be achieved by regulating metal ions, ligands, solvents, reaction conditions, etc. [12].

At present, hydrothermal synthesis is the most commonly used method to prepare MOFs, which is more facile and controllable than those of stirring, ultrasonic (US), microwave, and mechanochemical synthesis [53]. Up to now, MOFs have been extensively studied including UIO (named by University of Oslo), zeolitic imidazolate framework (ZIF), porous coordination network (PCN), coordination pillared-layer (CPL), MIL (named by Materials of Institute Lavoisier), isoreticular MOF (IRMOF) series and their corresponding derived materials, etc. For the above properties, these nanostructures have been demonstrated to be effective for anti-*S. aureus* infection. Detailed discussion will be introduced in the following parts of this paper.

4 Evaluation of the antimicrobial activity

Commonly, *S. aureus* and MRSA are chosen as the model microorganism to evaluate the antimicrobial activities of MOFs. As shown in Fig. 1, dilution plate coating test is employed to determine the inhibition of MOF-based materials on bacterial growth. The obtained bacterial growth curve shows the trend and change of bacterial reproduction after MOF-based materials treatment. Minimum inhibitory concentration (MIC), minimum bactericidal concentration (MBC), and half maximal inhibitory concentration (IC50) of antibacterial agents can be applied as standard benchmarks to evaluate the effect and dosage of MOF-based antibacterial materials. The average inhibition diameters are applied to estimate the antimicrobial sensitivity of MOF-based materials. Scanning electron microscopy (SEM) and transmission electron microscope (TEM) images are employed to determine damage of cell membrane and relevant morphology. Live/dead bacterial staining test can be performed with a dark field microscope to estimate the proportion of viable bacteria. To verify that the MOF-based materials don't cause bacterial resistance, circulating antimicrobial test is needed to be performed. Besides, the crystal violet staining test is applied to evaluate bacterial biofilm growth inhibition.

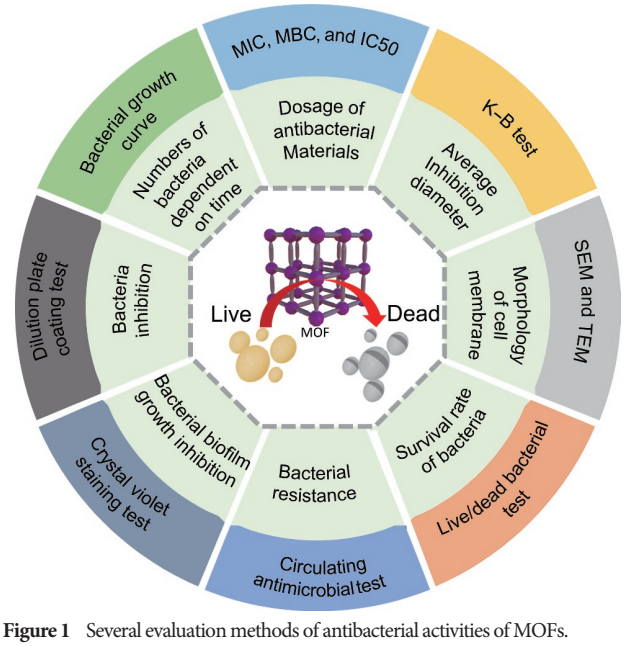

Figure 1 Several evaluation methods of antibacterial activities of MOFs.

4.1 Dilution plate coating test

Dilution plate coating test is a kind of counting method according to the culture characteristic of single colonies generated by microorganisms on solid medium. Generally, MOFs materials with different concentrations were mixed with a certain amount of bacterial suspension. Then plate coating was carried out after applied external conditions. After individual colony counting, the lethality of the materials against *S. aureus* was evaluated. The antibacterial efficiency can be calculated according to the following equation: antibacterial efficiency = (number of bacterial colonies in each group)/(number of bacterial colonies in the control group) × 100%.

4.2 Bacterial growth curve test

The bacterial growth curve test is employed to inoculate a small number of single-cell microorganisms into a certain volume of liquid culture medium. The above culture medium is conducted under appropriate conditions, and sampling is taken to determine the number of clones on schedule. After that, the curves can be achieved by using the logarithm of bacteria growth as the ordinate and culture time as the ordinate. Specifically, *S. aureus* was firstly cultured in Luria–Bertani (LB) medium. And then, a certain concentration of bacterial suspension was added into LB liquid medium containing different amounts of MOF-based materials. The bacteria were cultivated and the growth rates of *S. aureus* were monitored in a time-dependent manner [54].

4.3 MIC, MBC, and IC50

MIC is generally determined by broth microdilution assay. Nutrient broth, microorganisms, and the MOF-based materials were mixed and filled to a final volume of 200 μL using a 96 well microliter plate. It can be considered as the MIC when no visible turbidity on the lowest concentration of MOF-based materials after incubated for a certain time, confirming by turbidimetric or colorimetric-based test [55]. MBC refers to the required minimum concentration to kill 99.9% of the tested microorganisms [56]. IC50 refers to the measured semi-inhibitory concentration of an antagonist, indicating half of a drug or material that inhibits microorganisms.

4.4 The Kirby–Bauer (K–B) test

The K–B test can estimate the antibacterial activities of MOF-based materials by observing average inhibition diameter. It can be obtained by leaving MOF-based materials in an agar plate containing a certain concentration of bacterial suspension and then incubating [57]. Usually, the diameters of inhibition zone were measured under the same experimental condition and compared with those of MOF-based materials groups. When the above parameters were fixed, the antibacterial activities were presented as a mean of inhibition zone diameter (mm) ± standard deviation (SD).

4.5 SEM and TEM

Morphological observation can be obtained by using SEM or TEM, which can intuitively observe the survival status of bacteria and intact state of bacterial cell membrane. Hence, the SEM and TEM results of bacteria before and after treatment can be employed as an intuitive visual response of antibacterial effects. The preparation process of bacterial samples was conducted according to Ge's methodology, further for SEM observation [66].

4.6 Live/dead bacterial staining test

To further visualize the antibacterial effect, *S. aureus* was stained using the SYTO9/propidium iodide (PI) kit, containing two

fluorescent dyes of red-fluorescent PI and green-fluorescent SYTO9, which intercalate with DNA. SYTO9 is small enough to penetrate intact cell membranes, bind to DNA, and stain living cells with green fluorescence. PI is a red fluorescent dye with a high molecular weight and usually does not penetrate intact membrane of bacteria. If the cell membrane is damaged, PI crosses the membrane and then binds to the internal nucleic acid, together with the dead bacteria is infected by red fluorescence. Under the fluorescence microscope, the dead bacteria can be observed and directly counted according to the fluorescence color [67].

4.7 Circulating antimicrobial test

To detect the bacterial resistance, circulating antibacterial test can be performed. Typically, the first antibacterial process was conducted by using the dilution plate coating test as mentioned above. Then, the trace residual bacteria were collected and cultured in a constant temperature shaker with LB liquid medium for 12 h. After a lot of proliferation generated, the bacterias were diluted. Subsequently, the standard plate coating test was repeated for five cycles, verifying bacterial resistance to samples. In addition, the concentration of bacteria can be determined by regularly monitoring the OD600 of the remaining bacterial solution [68, 69].

4.8 Crystal violet staining test

Biofilms can be defined as microbial-derived sessile communities characterized by cells with a matrix, interface, or connection to each other [70]. It embedded in an extracellular polymer matrix and exhibited altered phenotypes in growth, gene expression, and protein production. The crystal violet staining test was applied to evaluate bacterial biofilm growth inhibition and eradication effect by using optical density of CV-stained biofilm suspensions [71].

5 Antibacterial mechanisms of MOFs

As shown in Fig. 2, the antibacterial mechanisms of MOFs are generally related to their chemical properties/structure and can be divide into metal ion releasing system, MOFs as carrier of antibacterial drugs, and oxidative stress. The antibacterial mechanism according to oxidative stress can be further subdivided into catalytic reactions based on chemical substances and oxidative stress reactions depended on external energy conversion. In this chapter, the antimicrobial mechanisms of MOFs are reviewed in detail.

5.1 Metal ion sustained-release systems

A large part of metallic elements have been widely used in antibacterial materials due to their multiple chemical properties, particularly in the synthesis of metal cluster derived MOFs. Although the exact mechanisms of antibacterial action of nanomaterials were unknown for most of history, recent research suggests that the concepts of bioinorganic chemistry and toxicology may provide an insight into how metals damage and kill pathogens. Through interaction, metal ions can bind to the atoms of donor ligands, such as O-, N-, and S- [72, 73]. These interactions depend on coordination chemistry and are the binding forces of hydroxyl, carbonyl, carboxyl, amino, and sulfhydryl groups in bacterial cell membranes.

In addition, the coordination stability between metal and ligand is related to the hard and soft acid-base (HSAB) theory [74]. Soft acids (e.g., Ag^+, Cu^+, Hg^{2+}, and Cd^{2+}) and critical acids (e.g., Co^{2+}, Ni^{2+}, Cu^{2+}, and Zn^{2+}) have large ionic radii, low oxidation states, and strong polarization. Therefore, they prefer to bind closely to soft bases, such as the mercapto group found in proteins [75, 76].

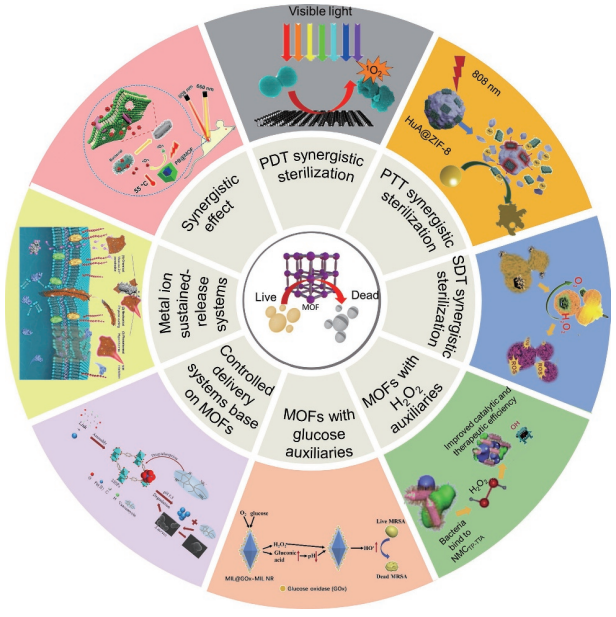

Figure 2 Classification and antibacterial mechanisms of MOFs. PDT synergistic sterilization: Reproduced with permission from Ref. [58], © American Chemical Society 2018. PTT synergistic sterilization: Reproduced with permission from Ref. [59], © Elsevier B.V. 2020. SDT synergistic sterilization: Reproduced with permission from Ref. [60], © American Chemical Society 2019. MOFs with H_2O_2 auxiliaries: Reproduced with permission from Ref. [61], © Wiley-VCH GmbH 2020. MOFs with glucose auxiliaries: Reproduced with permission from Ref. [62], © Elsevier B. V. 2020. Controlled delivery systems based on MOFs: Reproduced with permission from Ref. [63], © American Chemical Society 2017. Metal ion sustained-release systems: Reproduced with permission from Ref. [64], © American Chemical Society 2019. Synergistic effect: Reproduced with permission from Ref. [65], © American Chemical Society 2019.

Hard acids generally possess small ionic radii, high oxidation states, and weak polarization. They tend to form stable metal-organic complexes when paired with hard bases with high electronegativity.

According to HSAB theory, MIL-53(Al), MIL-100(Al, Fe, Cr), MIL-101, and UIO-66 were successfully synthesized [77, 78]. Because MOFs with strong water stability will expose multiple metal active sites, the electrostatic interaction between cationic metal and anionic cytoderm of bacteria will lead to cytoderm and cytomembrane damage and inactivation of pathogens [16]. For example, it has been shown that the electrostatic interaction of Ag^+ can severely damage the cytoderm of *S. aureus*, affecting the normal metabolism of the bacteria [79]. Recent studies have further shown that the transport of correct metal ion cofactors can be inhibited in intracellular proteins through competition when metal ions accumulate to a certain toxic dos [80]. Consequently, it affects bacterial function and leads to DNA damaging, denaturing and enzyme inactivation.

5.2 Controlled delivery systems based on MOFs

Antibiotics are encapsulated in MOFs with diverse properties and released spontaneously or controlled by external stimuli. The release mechanisms are generally classified as targeting cytoderm's structure, cytomembrane's function and structure, folic acid synthesis, DNA structure and function, and protein synthesis [81]. Some representative examples can be listed as follows:

(I) In a low osmotic environment, the synthesis process of cell wall mucin can be inhibited by the release of β-lactam containing antibiotics from MOFs, further destroying cell wall integrity and causing bacterial swelling, rupture, and death.

(ii) The interaction between polymyxin B antibiotics and bacterial cell membrane will destroy the integrity of outer

membrane. It also enhances the permeability of cell membrane due to the opened ion channels, leading to the escape of small molecules such as phosphate and nucleoside in cytoplasm, resulting in cell dysfunction and death.

(iii) Sulfa and trimethoprim antibiotics released by MOF are taken up by bacteria and then inhibit the enzymes responsible for folic acid synthesis. The released antibiotics are the important precursors during thymidine synthesis, thereby destructing the production of nucleic acid.

(iv) The released quinolones and nitroimidazole antibiotics inhibit bacterial DNA from forming super-helical cells and damage chromosomes, thereby killing bacteria.

(v) Aminoglycoside antibiotics released by MOF can affect the whole synthetic process of bacterial protein. It also hinders the process of initial complex synthesis, induces bacterial synthesis of wrong proteins, and inhibits the release of synthesized proteins, thus leading to bacterial death [81, 82].

5.3 Catalytic system based on oxidative stress

Another important mechanism of the antimicrobial activity of MOFs is generated through the oxidative stress. This process can be divided into two types, namely reactive oxygen species (ROS) dependent and ROS independent. Toxic ROS produced by MOFs and its derived nanomaterials, including superionic radical ($\cdot O_2^-$), hydroxyl radical (·OH), hydrogen peroxide (H_2O_2), and singlet oxygen ($^1O_2$), are important strategy to kill bacteria. Studies have proved that ROS is an important substance in organisms and can resist the damage of bacteria, fungi and parasites to the human body [83]. The reason is that toxic ROS can induce protein damage of pathogens, lipid peroxidation of cytomembrane, mitochondrial dysfunction and cytoderm shrinkage, and then cause the final death of pathogens [84]. MOFs can produce ROS without additional energy input after the treatment of chemical additives, such as H_2O_2 and glucose.

In fact, different types of antibiotics can activate the typical tricarboxylic acid cycle (TCA) cycle. The over-activation of electron transport chain induces the formation of superoxide and H_2O_2, which destroys the iron-sulfur clusters and thus destabilizes Fe^{2+}. Unstable Fe^{2+} can further react with H_2O_2 in Fenton reaction, leading to the production of ·OH that damages DNA, lipids, and proteins [85]. In addition, $\cdot O_2^-$ reduces Fe^{3+} produced by Fenton reaction to Fe^{2+}, avoiding excessive $\cdot O_2^-$ attacking the enzyme containing iron and sulfur clusters, while Fe^{2+} catalyzes Haber–Weiss reaction ($\cdot O_2^- + H_2O_2 \rightarrow OH^- + O_2 + \cdot OH$), thus forming more ·OH. Due to the short half-life, strong oxidation potential and lipid insolubility of hydroxyl radical, it brings with irreversible oxidative damage to the nearby nucleic acids, proteins, and fats [86]. Therefore, recently researchers have considered H_2O_2-assisted MOFs strategy as promising alternative for antimicrobial application. In addition, in the presence of glucose, glucose oxidase (GO_x) can continuously generate H_2O_2 and gluconic acid *in situ*, realizing a cascade catalytic reaction.

5.4 Energy conversion based bactericidal mechanism

Compared with chemical-assisted catalytic therapy, the synergistic approach triggered by external energy exhibits more significant bactericidal efficiency and higher selectivity than locally catalyzed bacterial therapy. At the same time, it minimizes risks, such as bacterial resistance result from conventional sterilization method. According to the different forms of external energy, the antibacterial mechanism is divided into photoelectric effect, photothermal effect, and ultrasonic treatment.

5.4.1 Photodynamic effect

Photoexcited triplet photosensitizers (PS) can react in two forms: (I) through hydrogen or electron transfer, react directly with substrates or solvents to form free radicals; (II) energy is transferred to oxygen molecules, forming $^1O_2$.

Through type I and type II reactions, a series of toxic active products represented by $^1O_2$ can react with biological macromolecules such as phospholipids, nucleic acids, and proteins of cells or microorganisms, destroy the structure of biofilm or other functional units, and make cells or microorganisms die, thus achieving therapeutic effects. At the beginning of the 20th century, people have discovered several substances that can be used as photosensitizers, such as acridine propyl yellow, acridine yellow, triphenylmethane, crystal violet, and bright green. Although they exhibited superior optical properties, but still possessed some defects such as low hydrophilicity, strong toxicity, and weak biodegradation. Surprisingly, MOFs have been used as ideal nanomaterials for anti-infection of phototherapy nanoplatforms due to their advantages of adjustable structure, easy modification, high specific surface area, permanent pores, and good biocompatibility.

5.4.2 Photothermal effect

Photothermal disinfection depends on the local high temperature generated by the photothermal conversion agent (PTA) under near-infrared (NIR) laser irradiation, leading to the death of bacteria. It is taken for an effective antibacterial strategy with high selectivity, low side effects, short treatment duration, and noninvasiveness. The principles of photothermal conversion include: (1) The electron relaxation of the excited state decays back to the ground state, causing the chromophore to collide with the surrounding environment, and part of the energy is released in the form of heat. The representative materials are carbon nanomaterials. (2) The light guides the polarization of free electrons, and the accumulated charge depolarizes, leading to collective electron oscillation, attenuation of surface plasma transition, and dissipation of energy in the form of heat. This mode is called "in-band transition". The representative high carrier density materials include precious metals such as gold and silver. (3) Semiconductor has conduction band and valence band, conduction with electrons, and valence band without electrons. When the semiconductor is illuminated with high-energy light, electrons are excited to the higher energy levels in the conduction band and it leaves holes in the valence band. Electrons and holes will relax to the band edge by vibrational relaxation, causing a thermalization process that converts energy into heat. The conversion generally occurs on low electron density materials.

Benefit from the advantages of NIR, the development of a series of photothermal nanomaterials with strong light absorption has become the focus of people's attention. Because these materials convert light energy into heat, the heat produced not only inhibits the development of drug-resistant bacteria but also prevents the formation of biofilms. Most studies on photothermal spectroscopic analysis of nanomaterials fall into: carbon-based nanocomposites [126, 127] (e.g., graphene derivatives), noble metal nanocomposites (e.g., gold, silver) [128], metallic nanocomposites (e.g., molybdenum sulfide) [129], and polymers and other nanostructures (e.g., polyaniline and liposomes). This classification is based primarily on their principal components in converting light energy into heat. MOFs have attracted much attention because of their semiconductor-like behavior, controlled porous structure, and large surface area. The porous nature gives MOFs special advantages and allows for additional functions through pore space engineering [130]. By integrating the synergistic advantages of MOFs and photosensitizers, guest materials (such as metal NPs) can be easily introduced into MOFs to improve the photothermal properties.

5.4.3 Sonodynamic effect

As for sonodynamic therapy (SDT), the exact antibacterial mechanism is still under debate, but many studies have fully demonstrated its efficacy. It is widely believed that sonosensitive nanomaterials themselves can act as sound sensitizers and produce toxic ROS in SDT, which is the main killing effector of bacteria. At present, sonoluminescence and sonochemical pyrolysis have been proposed to activate the acoustic sensitizer to produce ROS. The concept of sonoluminescence refers to the creation of bubbles in a liquid, which then collapses into a very small volume with an internal temperature of more than 100,000 degrees Celsius, giving a flash of light in the process [131]. Sonochemical pyrolysis refers to raising local temperature and pressure through cavitation processes, further decomposing sonosensitizer to produce free radicals [132]. It has been reported [133] that MOF and MOF-derived materials can be used for SDT treatment as efficient inorganic sonosensitizers, overcoming the problems of poor solubility of traditional organic sonosensitizers in water, easy elimination from blood circulation, and low accumulation in the lesion site, and enhancing the sonodynamic treatment effect. ROS have the potential to be hypogenic mutagenic due to their non-specificity, whereas SDT is effective against almost all microorganisms without concern for drug resistance. Second, ultrasound is topical and non-invasive, so it can avoid tissue toxicity caused by traditional antibacterial drugs.

5.4.4 Synergistic effect

The multi-mechanism synergistic effect is more attractive and effective in enhancing antibacterial activity. In MOF-based nanomaterials for antimicrobial applications, photothermal therapy (PTT) and photodynamic therapy (PDT) are commonly employed to investigate the synergistic effects. Photothermal effects, local hyperthermia, and additional oxidative stress generated by PDT assist single MOFs to release metal ions, ligands and antibacterial drugs, which greatly accelerate the antibacterial effect and even eradicate target microorganisms. In addition, various kinds of MOFs and photosensitizers also can be directly used for photothermal disinfection and PDT.

6 Metal ion sustained-release systems based on MOF materials

MOFs have been widely reported as a structure for the controlled release of antimicrobial agents [52, 134]. Nevertheless, most MOFs with weak coordination bonds between metal clusters and ligands in aqueous conditions cause severe drawbacks such as low stability, low water affinity, frameworks easily collapse, thus limiting their further extensive application [135–137]. In the 1990s, the as-synthesized MOF-5 could retain the integrity of the skeleton, thus becoming a representative in the development of MOFs [49]. Subsequently, the stability of MOFs can be strengthened by synthesizing nitrogen-containing MOFs, MOFs with a high coordination number, or modification of organics during post-synthesis [138]. A variety of metal ions have been reported to synthesize MOFs with diverse antibacterial activity [63, 139]. According to the unique properties, MOFs with bactericidal efficacy can be fabricated by exploiting the antibacterial properties of active antibacterial components. As MOFs break down, these components are slowly and constantly released to achieve long-term antibacterial effects [140–142]. Table 1 summarizes constitutes, synthetic methods, and bactericidal mechanism of various MOFs and MOF-based composites. In this review, four common metal ions (Cu, Zn, Ag, and Fe) were introduced and discussed. We would like to mainly focus on the preparation of MOF-based nanomaterials and the corresponding anti *S. aureus* application.

6.1 Cu-based MOF materials

Copper ion (Cu^{2+}) is an essential trace element for the maintenance of bioactivity, which exhibits chemically stable and low toxic properties. In addition, Cu^{2+} plays a vital role in activating cell energy production, regulating metabolism, resisting aging, synthesizing elastin, and forming human nerve tissue, which makes it become a widely used long-term antibacterial materials [143–145].

Recent studies showed Cu-based MOF materials could kill *S. aureus* by releasing Cu^{2+} with strong antibacterial activity [146]. The reported Cu/1,3,5-benzenetricarboxylic acid (Cu/H_3BTC) MOF, self-assembled with Cu^{2+} and 1,3,5-H_3BTC, exhibited significant antibacterial ability. This study demonstrated the strong antibacterial activity was ascribed to Cu^{2+} together with the carboxylic group in organic part. In addition, another Cu-based MOF (HKUST-1, known as MOF-199 or $Cu_3(BTC)_2$) is a classical and the most recognized MOF with square-shaped pores [147]. However, its further practical application is limited due to the water instability and inherent powder properties. To overcome these obstacles, immobilizing the MOFs on polymers and textiles (such as fibers, polyacrylamide, chitosan (CS), and cotton) is deemed as an effective way [148–150].

In a study, Cu-MOF nanostructures were formed on surface of silk fibers by using alternating plating solution layering techniques. The obtained CuBTC MOF showed high antibacterial activity against *Escherichia coli* (*E. coli*) and *S. aureus* [148]. Another study further demonstrated that Cu-BTC based on the *in-situ* formed polyester (PET) and nylon exhibited outstanding antibacterial performance towards different microbial pathogens including *E. coli*, *S. aureus*, and *C. albicans* [151]. In addition, versatile CS is one of the most attractive options due to its intrinsic antibacterial, biodegradable and hemostatic activity. Ren et al. [89] reported an antibacterial film composed of CS and HKUST-1 as a multifunctional antibacterial platform, which can slowly release Cu^{2+} ions and reduce the cytotoxicity (Fig. 3(a)). As shown in Fig. 3(b), Wang et al. presented the HKUST-1/chitosan/PVA fibers by using electrospinning, which presented good antibacterial activity against *E. coli* and *S. aureus* with 99% antibacterial efficiency [92].

The ROS production ability of energy-sensitive MOFs can be activated or boosted by introducing an additional energy source such as light and ultrasound [155]. Han et al. [95] constructed a Cu-based MOF material by introducing Cu^{2+} into the porphyrin ring of PCN 224, which improved the photocatalytic property and the yields of ROS. This can be attributed to the trap electron ability of Cu^{2+}, thus suppressing electron–hole recombination land accelerating the carriers transfer (Fig. 3(c)). Doping with 10% Cu^{2+} endows MOFs the high antibacterial efficiency against *S. aureus* (reach to 99.71% within 20 min) due to the synergistic effects of ROS and heat (Fig. 3(d)). Ultimately, the Cu^{2+}-MOFs can effectively kill *S. aureus* and treat wound infection *in vivo* experiment.

6.2 Zn-based MOF materials

Zn^{2+} is a divalent cation that acts as a cofactor for various enzymes, which is widely used in catalysis, structure, and regulation in human body. As show in Fig. 4(a), Fan and co-workers [64] developed the thermally responsive brushes (TRB)-ZnO@G composite, consisting of MOF-derived ZnO on graphene (ZnO@G) anchored with phase transformable TRB. The TRB-ZnO@G with flexible 2D nanostructures exhibited excellent photothermal activities and sustainable Zn^{2+} ions release. Compared with control group, ZnO@G/TRB-ZnO@G co-cultured groups showed incomplete bacterial membranes and Zn

Table 1 Summary of antimicrobial applications of MOFs and MOF-based composites based on the release of metal ions

Materials	Metal ions	Organic ligands	Synthetic methods	Bactericidal mechanism	Ref.
CHX@Cu-BTC	Cu^{2+}	H_3BTC	Mechanochemical	Cu^{2+} releasing	[87]
CuS@HKUST-1	Cu^{2+}	H_3BTC	Mechanochemical	Cu^{2+} releasing and PTT	[88]
HKUST-1/CS	Cu^{2+}	H_3BTC	Freeze-drying	Cu^{2+} releasing	[89]
MOF-199@PVDF	Cu^{2+}	H_3BTC	Mechanochemical	Cu^{2+} releasing	[90]
Cu-BTC/PVA	Cu^{2+}	H_3BTC	Mechanochemical	Cu^{2+} releasing	[91]
Pectin/PEO/F-HKUST	Cu^{2+}	H_3BTC	Mechanochemical	Cu^{2+} releasing	[67]
HKUST-1/CS/PVA	Cu^{2+}	H_3BTC	Mechanochemical	Cu^{2+} releasing	[92]
Pullulan/TBC/Cu-MOFs	Cu^{2+}	H_3BTC	Mechanochemical	Cu^{2+} releasing or generating ROS	[93]
SA-Cu(II)	Cu^{2+}	Succinic acid	Mechanochemical	—	[94]
Cu_{10}MOF	Cu^{2+}	H_4TCPP	Mechanochemical	PDT and PTT	[95]
Cu-TCPP(Fe)	Cu^{2+}	TCPP(Fe)	Mechanochemical	Generating ROS	[96]
Cu-BTC/GO	Cu^{2+}	Benzene tricarboxylic acid	Sonication	Cu^{2+} releasing	[97]
Cu-MOF NSs	Cu^{2+}	2-Methylimidazoie	Mechanochemical	PDT	[98]
PS@Cu-MOF	Cu^{2+}	Glutarate and bpa	Hydrothermally	Cu^{2+} releasing	[99]
Fe_3O_4@Cu-MOF	Cu^{2+}	2,6-Pyridine dicarboxylic acid	Mechanochemical	Cu^{2+} releasing	[100]
L-Glu-M-Cu(II)- MOF	Cu^{2+}	L-Glu	Mechanochemical	—	[101]
Cu-MOF-1/PLA membrane	Cu^{2+}	Citric acid	Electrospinning	Cu^{2+} releasing	[102]
Zn-BTC	Zn^{2+}	Trimesic acid	Mechanochemical	—	[103]
Zn-MOF	Zn^{2+}	4-Hydrazinebenzoate	Mechanochemical	Zn^{2+} releasing	[104]
BioMIL-5	Zn^{2+}	4-Bromophenacyl bromide	Hydrothermal	Zn^{2+} releasing	[105]
Zn-MOF/Ag	Zn^{2+}	2-Methylimidazole	Mechanochemical and calcination	Zn^{2+} releasing and PTT	[106]
$Zn_{50}Co_{50}$-ZIF	Zn^{2+}	2-Methyl imidazole	Mechanochemical	ROS generation	[107]
ZIF-8/GO-NH_2	Zn^{2+}	2-MIM	Mechanochemical	Zn^{2+} releasing	[108]
Ag NPs/Zn-MOFs	Zn^{2+}	4-bpdb and 2-NH_2-H_2BDC	Mechanochemical	Zn^{2+} releasing	[109]
Fe/SBA-16/ZIF-8	Zn^{2+}	2-MIM	Hydrothermal	Zn^{2+} releasing	[110]
$Zn_2(Bmic)_2(HAT)_2(DMF)_3$	Zn^{2+}	Tetrazole and 1-benzimidazole-5-carboxylic acid	Hydrothermal	Inhibition of biofilm formation	[111]
$Zn_3(BDC)_3(H_2O)_3.4DMF$	Zn^{2+}	Benzene-1,4-dicarboxylic acid	Mechanochemical	Zn^{2+} releasing	[112]
$[Zn_{2.5}(abta)(trz)_2(H_2O)]\cdot 3H_2O_n$	Zn^{2+}	1,4-Bis(benzimidazol-1-yl)-2-butene)	Mechanochemical	Inhibition of biofilm genes expression	[113]
$Zn(aip)(4,4'\text{-}bpy)_{0.5}(meoh)\}\cdot(H_2O)]_n$	Zn^{2+}	Aminoisophthalic acid and 4, 4′-bipyridine	Mechanochemical	ROS generation	[114]
Ag@MOF-5	Ag^+	1,4-Benzenedicarboxylic acid	Hydrothermal	Ag^+ releasing	[115]
$[Ag_2(Cedcp)]_n$	Ag^+	Ligand $h_3$cmdcpbr	Mechanochemical	Rupturing the bacterial membrane	[116]
Ag@MIL-53(Fe)	Ag^+	MIL-53(Fe)	Hydrothermal	Ag^+ releasing	[117]
AgNP@nanoMOF	Ag^+	Aminoterephthalate MIL-125-NH_2	Mechanochemical	Ag^+ releasing and ROS generating	[118]
Ag@MOF/CSNP	Ag^+	2-MIM	Hydrothermal	Ag^+ releasing	[119]
PLT@Ag-MOF-Vanc	Ag^+	2-Methylimidazole	Hydrothermal	Ag^+ releasing	[120]
Ag/MIL-101(Cr)/IMI	Ag^+	MIL-101(Cr)	Hydrothermal	Ag^+ releasing and ROS generating	[121]
$[Ag_2(O\text{-}IPA)(H_2O)\cdot(H_3O)]$	Ag^+	O-IPA	Hydrothermal	Ag^+ releasing	[122]
$Ag_2(\mu\text{-}PTA)_2(\mu\text{-}suc)]_n\cdot 2n\ H_2O$	Ag^+	PTA, succinic acid	Mechanochemical	Ag^+ releasing	[123]
Ag-MOF/polyamide thin-film	Ag^+	H_3BTC	Mechanochemical	Ag^+ releasing	[124]
Ag-MOF-polyamide thin membrane	Ag^+	2-Aminoterephthalic acid	Mechanochemical	Ag^+ releasing	[125]
MOF-53(Fe)@Van	Fe^{3+}	Terephthalic acid	Hydrothermal	Fe^{3+} releasing	[63]

elemental signal can be detected from the intracellular of bacteria based on TEM and energy dispersive X-ray spectroscopy (EDS) results (Fig. 4(b)). Especially, TRB-ZnO@G triggered by NIR caused the localized massive Zn^{2+} ions penetration, physical cutting, and hyperthermia killing, which synergistically enhanced the disruption of bacterial membranes and intracellular substances (Fig. 4(c)). Recent studies revealed that Zn^{2+} shows positive effects on promoting collagen deposition, cell migration, angiogenesis,

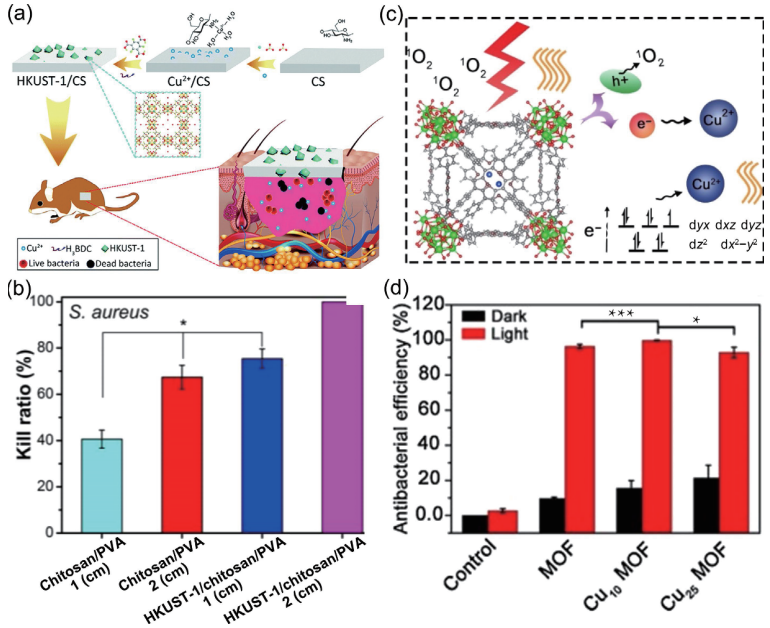

Figure 3 (a) Schematic of the HKUST-1/CS composite film and *in vivo* rat model. Reproduced with permission from Ref. [89], © Royal Society of Chemistry 2019. (b) Antibacterial activity against *S. aureus* of chitosan/PVA fibers and HKUST-1/chitosan/PVA fibers. Reproduced with permission from Ref. [92], © Elsevier B. V. 2020. (c) Schematic illustration of the mechanism of enhanced photocatalytic and photothermal ability of Cu^{2+} doped MOFs. (d) The statistical results *in vitro* of antibacterial activity of MOFs against *S. aureus* within 660 nm light for 20 min. (c) and (d) Reproduced with permission from Ref. [95], © Elsevier B.V. 2019.

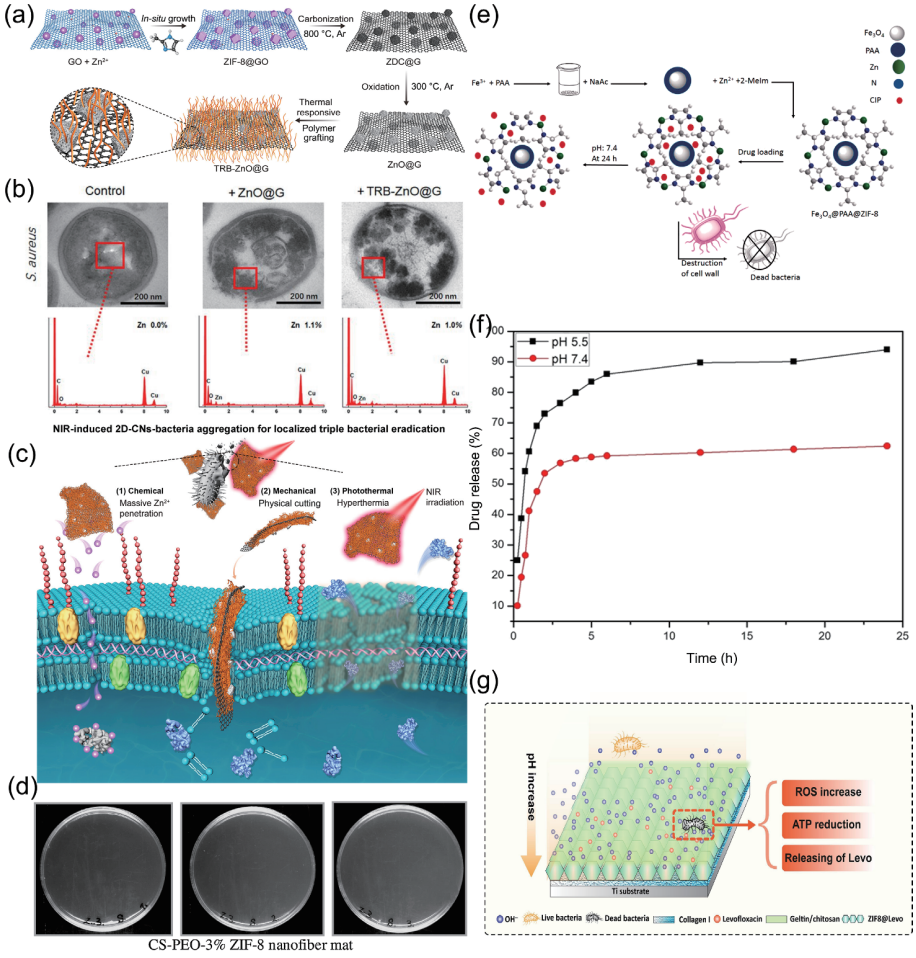

Figure 4 (a) Schematic illustration for the preparation of TRB-ZnO@G. (b) TEM images of the bacterial morphology and EDS patterns after co-cultured with different samples. (c) Proposed sustained and localized (Zn^{2+} penetration, mechanical, and photothermal) triple antibacterial activities of TRB-ZnO@G. (a)–(c) Reproduced with permission from Ref. [64], © American Chemical Society 2019. (d) The antibacterial activities of CS-PEO-ZIF-8 against *S. aureus*. The dilution from left to right is 1:50000, 1:500000, and 1:500000 respectively. Reproduced with permission from Ref. [152], © Elsevier B.V. 2016. (e) Simulation of the preparation of the Fe_3O_4@PAA@ZIF-8, drug loading, release, and antibacterial testing. (f) Release profile of ampicillin from ZnO@ZIF-8 particles in acetate (pH 5.5) and PBS (pH 7.4) buffer conditions. Reproduced with permission from Ref. [153], © Wiley-VCH Verlag GmbH & Co. KGaA, Weinheim 2019. (g) Schematic illustration of continuously release Levo and Zn^{2+} in ZIF-8@Levo/LBL. Reproduced with permission from Ref. [154], © Elsevier B.V. 2020.

fibroblast migration, and proliferation for wound healing [156–158]. Thus, the ZIF-8, as a result of stable tetrahedral clusters with Zn^{2+} and imidazole units as connecting chains, can be favorably employed for proteins encapsulation [159] and as drug delivery vehicles due to its high biocompatibility [160]. Iraj et al. [152] prepared antimicrobial chitosan polyethylene oxide (CS-PEO) nanofiber mats loaded with ZIF-8 NPs. The antibacterial activity of CS-PEO-ZIF-8 was assessed by a standard plate counting experiment, and the results showed that the antibacterial activity could reach 100% for food *S. aureus* (Fig. 4(d)).

Another characteristic of ZIF-8 is that it can be used to prevent bacterial colonization on drug delivery. ZIF-8 has shown excellent properties including thermal stability and pH-sensitive, regarding as a desired material for drug transfer [161]. As shown in Fig. 4(e), a novel magnetic framework of Fe_3O_4@PAA@ZIF-8 was prepared for the delivery of ciprofloxacin (CIP) antibiotic, which brings with a much higher antibacterial effect for *E. coli* and *S. aureus* [162]. The mechanism of antibacterial action is that CIP stopped DNA synthesis by inhibiting the effect of DNA gyrase in bacteria, further destroyed cell wall. A recent study further demonstrated that the antibiotic contained in core–shell structure of ZnO@ZIF-8 carrying ampicillin can be released in a controllable way through the pH response [153] (Fig. 4(f)).

To expand the practical applications, a great deal of research has been focused on the field of attaching MOFs to the supporting substrates [163]. To our knowledge, titanium (Ti) and its alloys are widely considered to be favorable substrate material in biomedical applications [164, 165]. As shown in Fig. 4(g), Lin et al. [154] developed a strategy for fabricating antibacterial coating on Ti with ZIF-8@Levo/LBL, which continuously released Levo and Zn^{2+}, resulting in increasing intracellular ROS levels in bacteria. Especially, the released OH^- from ZIF-8 surface reacted with H^+ from bacterial extracellular environment, drastically reducing the adenosine triphosphate (ATP) in bacteria. Hence, ZIF-8@Levo/LBL demonstrated intense antibacterial ability against *E. coli* and *S. aureus* through hydrolysis of ZIF-8 NPs. The ZIF-8@Levo/LBL also provides a new strategy for the development of multifunctional titanium implants in the treatment of orthopedic implant-related infections.

ZIF nanomaterials also have drawn greater attention for combating *S. aureus*-induced implant-associated infection. In order to avoid the *S. aureus* infection caused by implantation, a hybrid Mg/Zn-MOF74 coating was constructed on alkali-heat treated titanium (AT) surface [166]. The Mg/Zn-MOF74 coating also showed anti-inflammatory properties at early stage of implantation as well as the improved ability of new bone formation around implants. Recently, a TNT-ZIF-67@OGP was fabricated by coating ZIF-67@OGP (osteogenic growth peptide) on titanium dioxide nanotubes (TNTs) [168]. The multifunctional surface presented strong antibacterial activity against *E. coli*, *S. aureus*, *S. mutans*, and MRSA. This multifunctional implant combining osteo-immunomodulatory and antibacterial effects also provides a favorable material platform for implant-associated infectious bone regeneration.

6.3 Ag-based MOF materials

Both conventional silver and nano-silver with low toxicity and wide sterilization are approved by the U.S. environmental protection agency office for use as antibacterial agents [153]. Ag-based antibacterial agents with favorable antibacterial activity and wide antibacterial spectrum are generally used in the environment and human body [169]. Ag nanoparticles (NPs) exhibit high antibacterial activity but tend to spontaneously aggregate into large particles, which could not be uniformly dispersed in substrate [170]. Compared with Ag NPs, Ag-based MOFs can be considered as a reservoir for the gradual release of Ag^+, thus demonstrating antibacterial effect through the inherent bactericidal action of Ag^+ [171].

The reported Ag@MOF-5 nanoplates improved the dispersion of Ag NPs and the antibacterial activity [115]. Besides, the Ag/Ag_3PO_4 NPs incorporated in IRMOF-1 via hydrothermal approach showed good antibacterial properties for *E. coil* and *S. aureus* [167]. The antibacterial activity of Ag/Ag_3PO_4-IRMOF-1 was investigated by MIC and MBC experiments. Antimicrobial mechanism can be explained as follows: The photogenerated electrons of Ag/Ag_3PO_4-IRMOF-1 nanocomposite or Ag/Ag_3PO_4 nanoparticles are excited from the valence band to the conduction band with the irradiation of visible light, and the holes still remain in valence band. The photogenerated electrons are transferred to Ag nanoparticles to enhance the photocatalytic ability. Then photogenerated electrons could react with O_2 to generate $\cdot O_2^-$, which could directly decompose adsorbed *S. aureus* cells (Fig. 5(a)).

Huang et al. [120] reported a Ag-MOF based nano-drug delivery system. As shown in Fig. 5(b), the drug release and Ag^+ release of PLT@Ag-MOF-Vanc showed pH-responsive, which can inhibit the delivery system pre-releasing drugs in circulatory system. As shown in Figs. 5(c) and 5(d), the release rate of Ag^+ in a series of Ag-MOFs increased with the decreased pH value. Antibacterial experiments were carried out and it was found that PLT@Ag-MOF-Vanc exhibited a better antibacterial activity against common clinical strains including *S. aureus*. Especially, it targeted the MRSA-infected sites in the MRSA pneumonia model. The results also showed that PLT@Ag-MOF-Vanc did not give rise to obvious damage to the organs of Kunming mice because of its low toxicity *in vivo* and positive biocompatibility.

As displayed in Fig. 5(e), 3D and 2D Ag-based zwitterionic MOFs were synthesized with favorable water stability and solubility [116]. Its antibacterial property originated from the assembly of the quaternary ammonium carboxylic acid ligand in MOFs and Ag^+ ions, which strongly killed bacteria by continuous releasing Ag^+. The remarkable antibacterial activity was ascribed to the unique aromatic rings and positively charged pyridinium in ligands together with the continuously release of Ag+, thus resulting in powerful antimicrobial activity. In Section 2.5, we also point out that inhibition and elimination of biofilms formed by *S. aureus* is a major challenge. Recently, AgNP@nanoMOF was identified as an effective antibacterial agent to inhibit the spread of surface coating biofilm caused by *S. aureus* proliferation [118]. The relevant antibacterial mechanism further described the inherent bactericidal activity of MOF, the bactericidal property of Ag nanoparticles and photoactivity after ultraviolet light irradiation.

6.4 Fe-based MOF materials

Iron element involves in the synthesis of enzymes, regulation of energy metabolism, hematopoietic function, and immune regulation [173]. It was found that MOF-53(Fe) constructed by Fe ions and terephthalic acid showed good biocompatibility [174]. In addition, the framework of this material can be reversibly adapted to its pore size by drug adsorption and was highly stable in acidic environments [175]. Herein, MOF-53(Fe) was used as a drug carrier platform to encapsulate drugs and further synthesize MOF-53(Fe)@Vancomycin (Van), which can control drug release behavior under different pH and destroy *S. aureus* (Fig. 6(a)). As displayed in Fig. 6(b), SEM morphology of *S. aureus* showed the bacteria corrugated with distorted shapes and incomplete membranes when MOF-53@Van increased to 200 $\mu g \cdot mL^{-1}$. Meanwhile, free Van exhibited an enormous bacterial destruction. Additionally, as shown in Fig. 6(c), the Fe ions from the

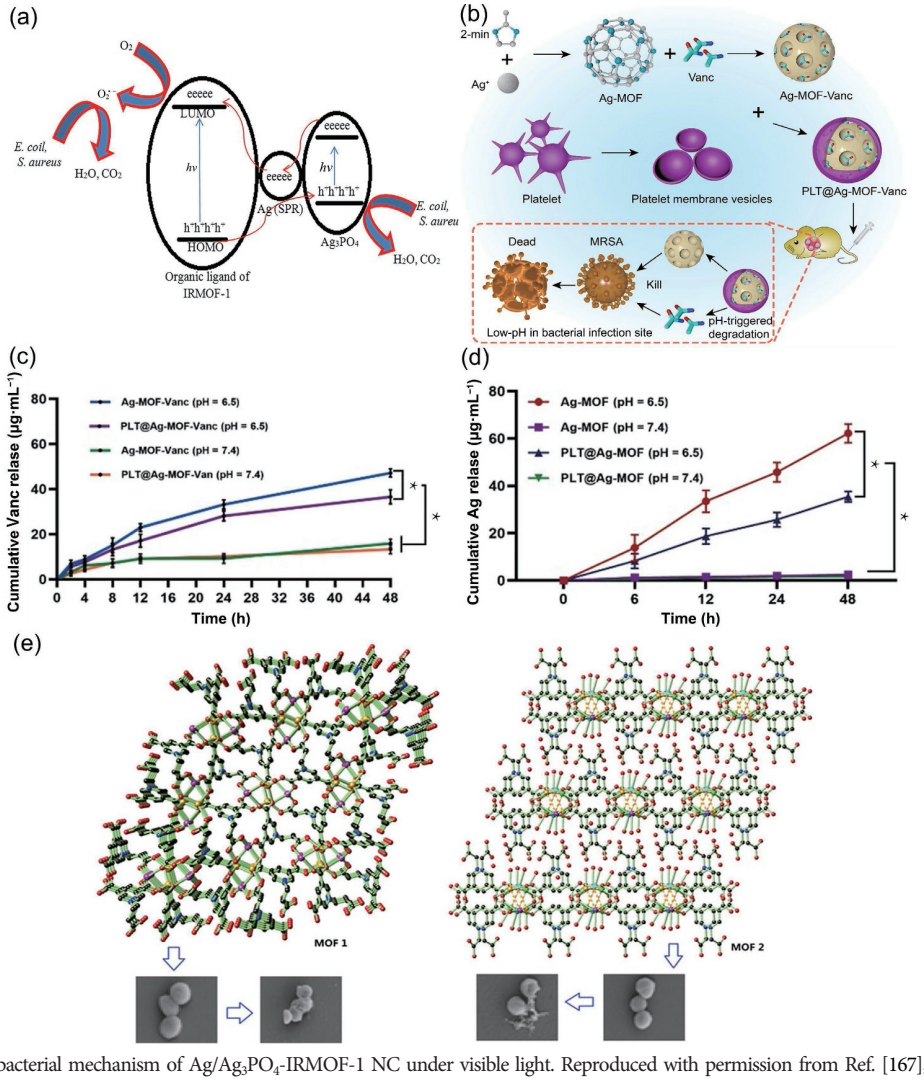

Figure 5 (a) Photo-antibacterial mechanism of Ag/Ag_3PO_4-IRMOF-1 NC under visible light. Reproduced with permission from Ref. [167], © John Wiley & Sons, Ltd. 2020. (b) Schematic diagram of PLT@Ag-MOF-Vanc in the treatment for MRSA infection. (c) Cumulative release rates of vancomycin from Ag-MOF-Vanc or PLT@Ag-MOF-Vanc at different pH values. (d) Cumulative release rates of Ag^+ from Ag-MOF-Vanc or PLT@Ag-MOF-Vanc at different pH values. (b)–(d) Reproduced with permission from Ref. [120], © Huang, R. et al. 2021. (e) 2D and 3D structure of Ag-based MOFs. Reproduced with permission from Ref. [116], © American Chemical Society 2020.

degradation of MOF-53(Fe) had been proven to be biocompatible [63]. Another novel strategy using MIL-100 (Fe) NPs as a nanocarrier for precise delivery of 3-azido-D-alanine was reported, which can be selectively integrated into the cell wall of bacteria [172]. With the assistant of PDT, the number of bacteria on infected skin tissue was dramatically decreased. As shown in Fig. 6(d), the results demonstrated the advantages of MOF-assisted bacterial metabolic labeling strategies in the accurate detection and treatment of bacteria under the guidance of fluorescence imaging.

7 Controlled delivery systems based on MOF materials

Loading or immobilization of antibacterial substances (gases, antibiotics, bactericides, antimicrobial NPs, etc,) on the surface or pores is a crucial method to endow devices with characteristic antibacterial properties [176]. There are two main approaches to load drugs into MOFs, including immersing synthetic MOFs in drug solutions and loading drugs during MOFs synthesis. Drugs and MOF are bound by van der Waals forces, electrostatic interactions, dipole interactions, hydrogen bonds, and π–π interactions [177]. The structure, morphology, and physical/chemical properties of MOFs can be controlled by optimizing constitutes and synthesis conditions, which endows great flexibility and plasticity for their application in drug delivery [178, 179].

Recently, CS and polyethylene glycol (PEG) polymers, antibiotic cephalexin (CFX) drug, and 0%–5% ZIF-8 NPs were prepared to construct a novel drug delivery system [180]. The blended nanocomposites exhibited good antibacterial properties of infectious wound and acceptable biotoxicity. As shown in Fig. 7(a), the 3-(4,5-dimethyl-2-thiazolyl)-2,5diphenyltetrazolium bromide (MTT) test suggested that films containing 0 wt.% and 1 wt.% of ZIF-8 NPs exhibited lower cell viabilities owing to more release of the CFX drug from the film than those of films including 2%–5% of ZIF-8. The previously mentioned MOF-53(Fe)@Van also can be deemed as a controlled delivery system [63]. The positively charged van was loaded onto negatively charged MIL-53(Fe) for sustainable release of van and made it applied for treating inflammation caused by implant-associated bacterial infection. The ratio of Fe^{3+} ions released from MOF-53(Fe)@Van to the total Fe^{3+} ions was related to the pH of the environment (Fig. 7(b)), while a small quantity of degradation of MOF-53(Fe) accelerated the release of van. Standard plate counting results showed that MOF-53(Fe)@Van exhibited the antibacterial activity of 99.3% against *S. aureus*. Ag NPs have been proven to be promising antibacterial material with better stability and low cost than traditional antibiotics, however, the excessive silver ions caused damage on healthy tissues [182, 183]. Ag NPs

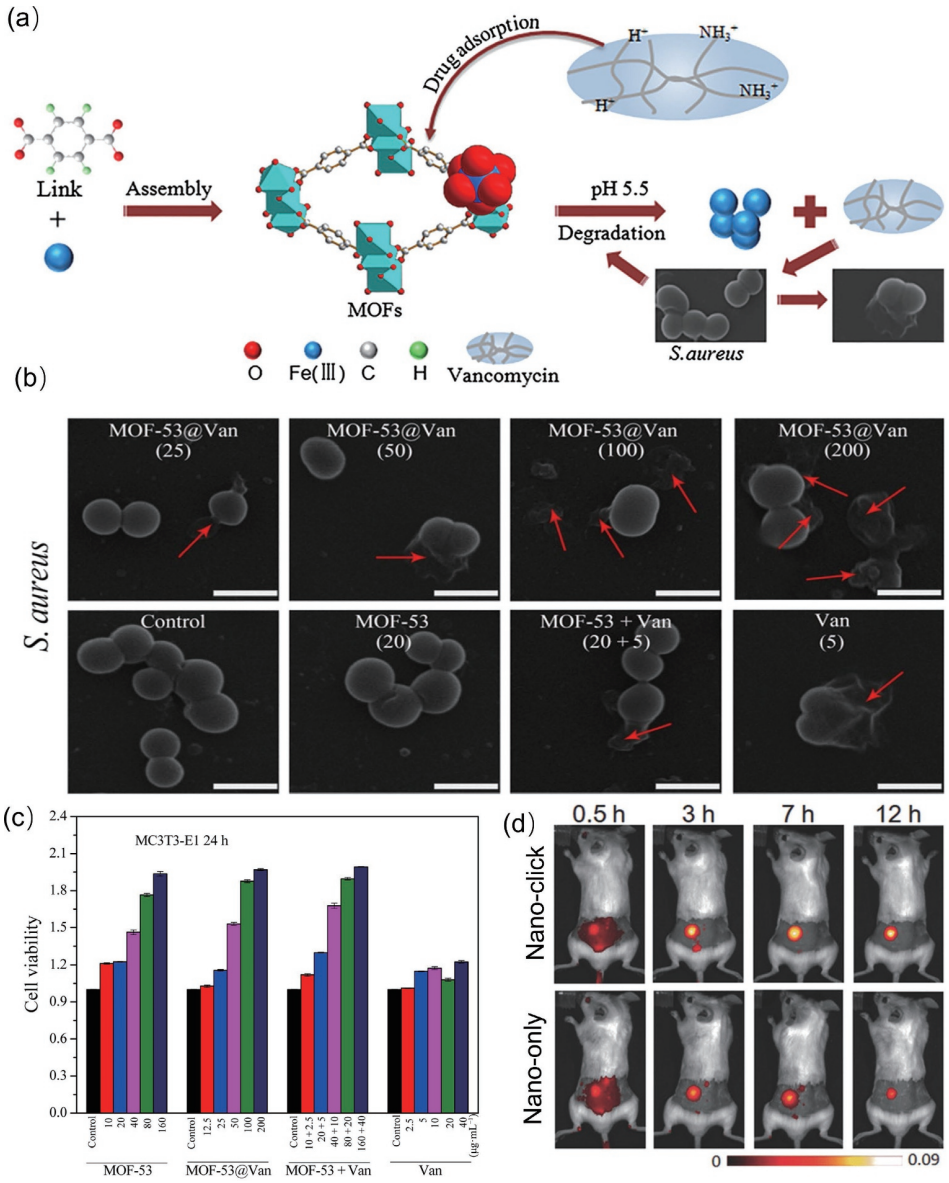

Figure 6 (a) Schematic representation of MOF-53(Fe) structure and the process of MOF packing drug molecules for killing bacteria. (b) SEM morphology of *S. aureus* seeded on various samples after incubation at 37 °C for 24 h. (c) MTT assay of MC3T3-E1 cell cultured with MOF-53, MOF-53@Van, MOF-53 + Van, and free Van for 24 h. (a)–(c) Reproduced with permission from Ref. [63], © American Chemical Society 2017. (d) Time-dependent *in vivo* fluorescence images of bacteria-bearing mice pretreated with d-AzAla@MIL-100(Fe) NPs (nano-click group) or saline (nano-only group), respectively, followed by i. v. injection of US-TPETM NPs (ultrasmall 2-(1-(5-(4-(1,2,2-tris(4-methoxyphenyl)vinyl)phenyl) thiophen-2-yl)ethylidene)malononitrile NPs). Reproduced with permission from Ref. [172], © WILEY-VCH Verlag GmbH & Co. KGaA, Weinheim 2018.

can be successfully encapsulated in spherical MOF to form Ag-Cu tetrakis(4-carboxyphenyl)porphyri (TCPP) MOF, which not only maintain the antibacterial activity of Ag but also avoid excessive release of Ag^+ ions and long-term direct contact between Ag and healthy tissues [184]. The obtained Ag-Cu TCPP showed a better antibacterial effect and lower cytotoxicity *in vitro* than those of penicillin. Duan et al. [181] reported a novel AgNPs@HKUST-1@CFs composite, in which Cu^{2+} ions coordinated with carboxyl methylated fibers (CFs) to achieve surface fixation of KUST-1, and then *in-situ* loaded with Ag NPs (Fig. 7(c)). The resulting AgNPs@HKUST-1@CFs greatly improved the dispersion and stability of Ag NPs, and effectively inhibited the upward growth of *S. aureus* by 99.41% (Fig. 7(d)). The antibacterial mechanism may include reducing the activity of bacterial membrane enzymes, destroying bacterial cell membranes, and inhibiting DNA replication [187].

Nitric oxide (NO) is related to the biological signal transduction pathway in human physiology and pathology, which may contribute to the incidence of infection by acting as a vasodilator, myocardial inhibitor, and cytotoxic agent. On the other hand, NO plays an essential roles in infected hosts due to the microvascular, cellular protective, immunomodulatory, and antibacterial properties [188]. However, delivering NO to the target in a controlled manner remains a significant challenge because of its high toxicity and short half-life. To this end, ordered nanoporous materials, including zeolite [189, 190], titanosilicates [191], and MOFs, have been proposed as NO delivery carriers in recent studies. The stability of MOFs endows the ability of NO storage and release [192]. It has been shown that the controllable and sustainable release of chemically stored NO in S-nitrocysteine can be achieved by using Cu-based MOF as storage carrier and catalyst [193]. Duncan et al. [194] further successfully prepared the NO-releasing CPO-27 as a model medical polyurethane, in which NO successfully encapsulated into the nanocomposite (Fig. 7(e)). During cytotoxicity tests, the nanomaterial showed a low toxicity. The membrane consisting of 5 wt.% MOF contributed a significant bactericidal effect on *E. coli* and *S. aureus* within 1 h demonstrating how polymer substrates control NO release in

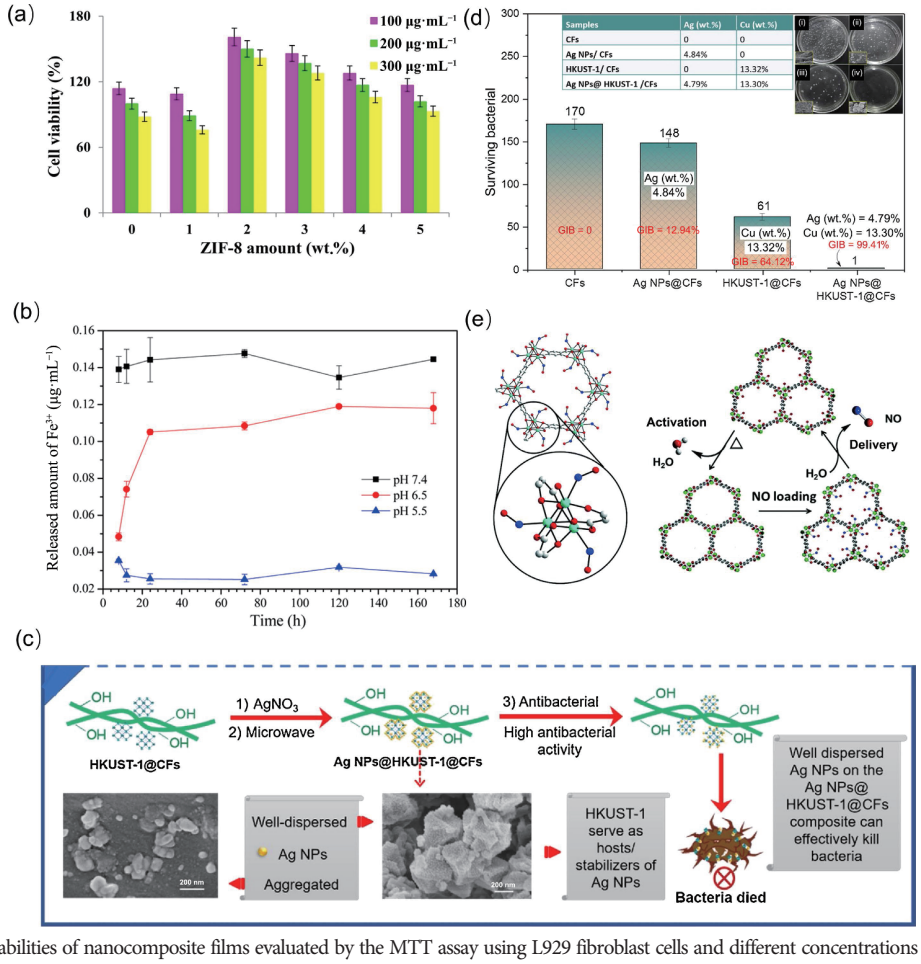

Figure 7 (a) The cell viabilities of nanocomposite films evaluated by the MTT assay using L929 fibroblast cells and different concentrations of the films. Reproduced with permission from Ref. [180], © Elsevier B.V. 2020. (b) Accumulated released amount of Fe^{3+} from MOF-53(Fe)@Van (100 μg·mL^{-1}) in different PBS solutions. Reproduced with permission from Ref. [63], © American Chemical Society 2017. (c) Schematic illustrations of synthesis of Ag NPs@ HKUST-1@CFs composites. (d) Photographs of bacterial colonies against of *S. aureus*. (c) and (d) Reproduced with permission Ref. [181], © Elsevier Ltd. 2018. (e) NO adsorption and release by CPO-27 MOFs.

MOF composites.

8 Catalytic systems based on MOF materials

ROS plays a crucial role in combating pathogens and causing biomaterial degradation [195]. For example, peroxidase (POD) can catalyze H_2O_2 to generate ·OH, which causes serious oxidative damage to pathogens [196]. However, the intrinsic disadvantages of natural enzymes such as high cost, complicated purification, poor stability, and difficulty of recycling have impeded their practical applications. Recently, MOF-based catalytic systems are mainly based on GOx, POD-, superoxide dismutase (SOD)-, and catalase (CAT)-mimetic activities or oxidase catalytic activities that catalyze O_2 to generate ROS like H_2O_2, $^1O_2$, and $\cdot O_2^-$ that significantly enhance antibacterial activity *in vitro* [197]. The potential catalytic activity of MOF materials can be improved by doping natural enzymes, enzyme-based cascade reaction properties, multi-enzyme catalytic properties, and single-atom catalytic properties. MOF-based catalytic systems emerge the characteristics of excellent activity, durability, and structural diversity, which bring with new properties of enhanced antibacterial performance to the development of MOFs [198, 199].

8.1 H_2O_2-assisted MOF materials

H_2O_2 has been widely used as a disinfection reagent. Due to its high oxidative stress, it disrupts the activity of biological components such as lipids, enzymes, and DNA, thus interfering with bacterial reproduction and metabolism. However, during bacterial disinfection, conventional H_2O_2 concentrations (0.5% to 3% by volume) hinder wound healing and even damage normal tissues [196, 200, 201]. It has been reported that nanomaterials such as V_2O_5 [202], Fe_3O_4 [203], and graphene quantum dots [200] can be used to assist H_2O_2 in antibacterial applications. For example, graphene quantum dots can catalyze the generation of ·OH from low concentrations of H_2O_2, which is highly bactericidal while avoiding the toxicity of high concentrations of H_2O_2. Unfortunately, peroxidase-like nanomaterials are intolerably cytotoxic due to their low catalytic efficiency and large leakage of metal ions [204, 205]. In recent years, H_2O_2-assisted MOF-based catalytic materials demonstrate great potential in combating bacterial infection.

Recently, due to their unique physicochemical and intrinsic enzyme-mimicking properties, MOF-based nanozymes open up a new avenue for constructing mesoporous nanozymes in both fundamental research and biomedical applications [206]. Zhang et al. reported a MOF@covalent organic framework (COF) nanozyme that has been designed as a high-efficiency peroxidase mimic [61]. Through a "sequential growth" method, the pseudopodia-like $COF_{(3,5\text{-triformylphloroglucinol (Tp)-(4,4',4''-(1,3,5-triazine-2,4,6-triyl) trianiline (TTA))}}$ ($CO_{FTP\text{-}TTA}$) grew on the POD like NM-88. Metal nodes and COFs were regarded as the active center and binding cavity, respectively, which formed a pore microenvironment for enrichment and activation of substrate molecules to enhance antibacterial effect. The antibacterial activity mechanism revealed the hybrid with pseudopod morphology can latch onto bacteria through a polyvalent topological interaction between the "hairy" bacteria and the prickly COF surface. H_2O_2 is the substrate and

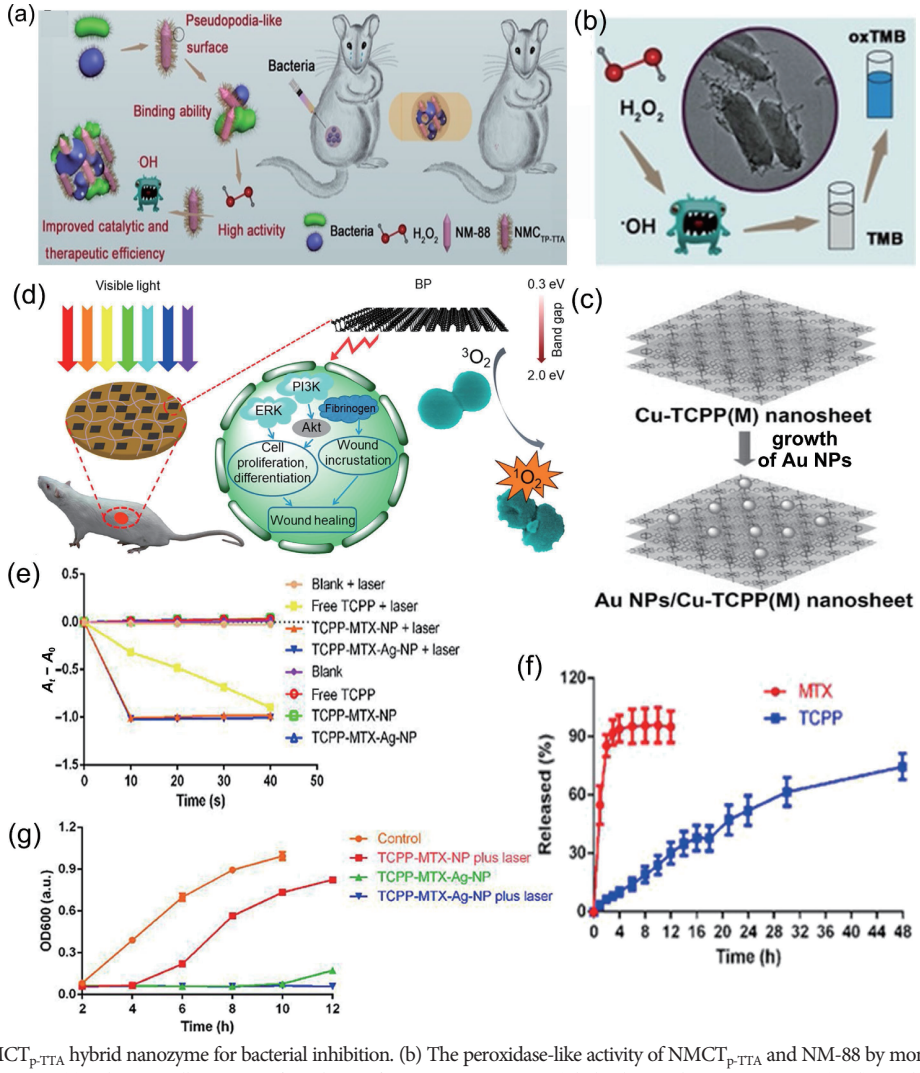

Figure 8 (a) Use of $NMCT_{p\text{-}TTA}$ hybrid nanozyme for bacterial inhibition. (b) The peroxidase-like activity of $NMCT_{p\text{-}TTA}$ and NM-88 by monitoring the absorption of TMB at 652 nm from pH 2–7. (c) Schematic illustration of synthesis of Au NPs/Cu-TCPP(M) hybrid nanosheets (M = Fe, Co). (d) Sterilization under visible light irradiation and the process of stimulating skin cell behaviors that can promote the regenerative activities of the skin cells and actively participate in skin regeneration to accelerate bacteria-accompanied wound healing using BP-based hydrogel. (e) The ROS generation measured by the DPBF method. (f) The release of TCPP and MTX from the TCPP-MTX-Ag-NP. (g) The bacterial growth profiles of the supermolecular nano-carriers. (a) and (b) Reproduced with permission from Ref. [61], © Wiley-VCH GmbH 2020. (c) Reproduced with permission from Ref. [185], © WILEY-VCH Verlag GmbH & Co. KGaA, Weinheim 2017. (d) Reproduced with permission from Ref. [58], © American Chemical Society 2018. (e)–(g) Reproduced with permission from Ref. [186], © American Chemical Society 2018. Feng, G. N. et al. 2021.

ultimately effectively kills bacteria through the *in-situ* produced ROS (Figs. 8(a) and 8(b)). In addition, the as-synthesized MOF@COF nanozyme can effectively treat wound infections and accelerate wound healing by eliminating *S. aureus*. In this regard, the research of MOF-based nanozymes for bacterial theranostics is becoming popular throughout the world when compared with natural enzymes and conventional MOF-based materials. Owing to the more easily synthesized, highly stable, and durable, these advantages will effectively push forward to the exploration of MOFs with enzyme-mimics properties for biomedical applications [207].

Various strategies also have been developed to further enhance the catalytic efficiency of MOF-based systems by adjusting components, decreasing their size, alloying, or synthesizing high refractive index nanocrystals. For example, as shown in Fig. 8(c), Huang et al. [208] developed Au NPs/Cu-TCPP(Fe) with excellent POD-like activity for antibacterial therapy of infectious wound, which was prepared by growing UsAuNPs on ultra-thin 2D Cu-TCPP(Fe). The enhanced enzyme-like activity can be attributed to the synergistic effect of Au NPs and Cu-TCPP(Fe). The construction of Au NPs on Cu-TCPP(Fe) exposed more catalytic active sites, which greatly improved the catalytic performance toward H_2O_2 decomposition into toxic·OH [185]. In addition, due to its ultra-thin thickness, 2D Cu-TCPP(Fe) can also reduce the mass transfer resistance of catalytic reactions.

8.2 Glucose-assisted cascade enzymatic reactions

Another attractive trend in literature has focused on MOF-dependent catalytic systems encapsulate GO_x and POD for cascading enzymatic reactions. With GO_x as the prototype enzyme, it is usually used in enzyme cascade catalysis, especially in blood glucose monitoring and a variety of enzyme reactions [209]. In this system, GO_x continuously catalyzes glucose to create rich gluconic acid and H_2O_2, thus avoiding the damage of non-local H_2O_2 addition.

For instance, a 2D Cu-TCPP(Fe) and GO_x nanocomposite was designed for effective antibacterial application and wound healing [96]. The physical adsorption of GO_x catalyzed the continuous conversion of glucose into rich gluconic acid and H_2O_2, which avoided direct use of higher concentrations of toxic H_2O_2 and minimized detrimental side effects. The resulting gluconic acid can reduce the pH value, significantly activating the peroxidase-like activity of Cu-TCPP(Fe). It's worth noting that the self-activated cascade antibacterial agent possessed high antibacterial activity against both of *E. coli* and *S. aureus*. Wang et al. [210] also

obtained a MOF-enzyme hybrid self-activated cascade antibacterial agent (GO_x/FeNi-MOF) by loading GO_x into FeNi-MOF, in which FeNi-MOF played a bi-functional role on peroxidase mimic and protective coating.

Similarly, GO_x was also used to load in a variety of POD-like MOFs, such as NH_2 -MIL-88B(Fe) [211], NH_2-Fe-MOF [212], (Fe) MOF-545 [213], and ZIF-8 [214] for biological applications. The amino-functionalized POD-like NH_2-MIL-88B (Fe) model was constructed with ligands containing basic (triazine) and weak acid (phenol) functional groups, endowing the material closer to natural enzymes. These synthesized MOF-based catalytic systems showed outstanding enzymatic cascade performance and may contribute to design the synergistic natural enzymes with high catalytic performance, further providing ideas for the application of MOF-based nano-enzymes. To address the persistent infections caused by biofilms, glucose-assisted cascade enzymatic reactions also played a key role in eliminating biofilm. In this regard, GO_x in MIL@GO_x-MIL NRs cut off the energy supply of MRSA biofilm by catalyzing glucose oxidation [62]. It also catalyzed the production of gluconic acid to reduce the pH in the environment, thus enhancing the activity of MIL nanoenzyme and continuously producing H_2O_2 to inhibit the formation of biofilm.

9 Energy Conversion systems based on MOF materials

Compared with the traditional catalytic bacterial therapy, the synergistic approach of exogenous energy shows higher bactericidal efficiency and minimizes the bacterial resistance and other risks. Exogenous energy can be triggered in the form of light, heat, sound, etc. PDT is a method of producing ROS through certain therapeutic agents using photosensitizers and excitation sources [218, 219]. PTT refers to a treatment that kills pathogens by using materials with high photothermal conversion efficiency and converting light energy into heat energy under exposure to an external light source. Surface chemical thermodynamics (SCT) utilizes ultrasound to penetrate biological tissues, especially focused ultrasound, which can focus sound energy into deep tissues without trauma and activate some sonosensitive drugs (such as hematoporphyrin) to produce antibacterial and anti-tumor effects. Compared with traditional chemotherapy and radiotherapy, phototherapy is less invasive, highly selective, and minimally damaging to normal tissues [220]. In recent decades, numerous studies are devoted to apply PDT, PTT, and SCT into the treatment of cancer and bacterial infection, achieving good therapeutic effects [221]. Hence, the synergistic approach of exogenous energy triggering shows great prospects as an emerging treatment method [222, 223].

9.1 PDT based on MOF materials

ROS was produced by using PS through irradiating with a certain wavelength of light, resulting in bacterial membrane shrinkage and rupture, tissue damage, and bacterial death. The generation of $\cdot O_2^-$ was dependent on the tricarboxylic acid cycle, then destroyed the iron-sulfur cluster in the protein and released Fe^{2+}, which in turn reacts with H_2O_2 to release ·OH (called the Fenton reaction). The product of $\cdot O_2^-$ binding with ·OH causes damage to bacteria's proteins, lipids, and nucleic acids [224]. Generally, zinc oxide [68], quantum dots [225], black phosphorus (BP) [226], copper sulfide [88], and graphite carbon nitride (g-C_3N_4) [227] can be used as PSs. Although the PSs show superior optical properties, they still have some defects such as low hydrophilicity, strong toxicity, and weak biodegradation [228–230]. Owing to their high surface area and periodic porous structure, the intrinsic photodynamic or photothermal MOF can be constructed by directly acting as PS or regularly wrapping PS molecules in the skeleton. It effectively decreased the self-aggregation and self-quenching of PS, improved water solubility, and maximizedd the utilization rate of light. Therefore, MOFs have received broad attention as an ideal nanomaterial for anti-infection using of light therapy nanoplatforms.

Although some studies were combined with the use of photosensitive BP to achieve effective sterilization, non-specific ROS may cause damage to normal cells and tissues (Fig. 8(d)) [58]. To treat bacterial infections by combining the antibacterial effects of PDT and Ag with the anti-inflammatory effects, Fu et al. [186] constructed a photosensitizer consisting of meso-TCPP, methotrexate (MTX), gallic acid (GA), and Poloxamer 407. These components were self-assembled into TCPP-MTX-NP nanostructure, and then Ag-doped TCPP-MTX-Ag-NP was further modified by silver through GA reduction reaction. As shown in Fig. 8(e), the ROS generation test showed the TCPP, TCPP-MTX-NP, and TCPP-MTX-Ag-NP displayed a stable visible absorbance without laser exposure, which suggested the laser alone or the nanoparticles alone would not produce ROS. As shown in Fig. 8(f), the MTX showed a rapid release from the TCPP-MTX-Ag-NP, however, the TCPP exhibited a slow release. At the same time, the photoresponsive MOF can generate singlet oxygen under visible light and cooperate with PDT to improve the sterilization efficiency (Fig. 8(g)).

9.2 PTT based on MOF materials

Different from PDT, PTT achieves synergistic sterilization by locally inducing high temperature. Hyperthermia can cause protein denaturation and aggregation, cell membrane shrinkage and rupture, affect DNA replication, affect cell function and eventually lead to cell inactivation. When the high temperature caused by PTT is too high to completely remove bacteria, non-local heating and high temperatures generally induce severe damage on healthy tissues [214]. The key to solve this problem is to realize synergistic antibacterial effect through PTT and appropriate treatment temperature design to achieve ideal antibacterial efficacy. The photothermal properties of PTT can be improved by carefully designing and constructing photosensitive MOF, that is to say, the MOF prepared by various doping methods can control its ability to capture light, which is helpful to acquire an in-depth understanding on mechanism of energy transfer.

Compared to visible light, NIR lasers are a better energy source for biocatalytic therapy with wavelengths in the 700–1,400 nm range because of their minimal tissue damage, their ability to penetrate mammalian bodies, and their great potential to induce synergies between PDT and PTT [231–233]. The synergistic triggering of PDT and PTT by NIR laser exchanges their unique but complementary therapeutic modalities to obtain desired antibacterial properties. As shown in Fig. 9(a), a NIR responsive nanocomposite (HuA@ZIF-8 NPs) was reported to exhibit concentration-dependent photothermal properties, which was constructed by adsorbing polyvinyl pyrrolidone (PVP) on the surface of HuA colloidal particles, and then encapsulated in ZIF-8 [59]. With the extension of irradiation time, the controlled release concentration of Zn^{2+} increased. The combination of Zn^{2+} and PTT achieved fast and effective sterilization. In addition, the NIR irradiated group showed higher antibacterial efficiency compared to the unirradiated group, and the concentration-dependent antibacterial activity of HuA@ZIF-8 NPs was demonstrated. The mortality rate of *S. aureus* reached 99.59% after 20 min NIR exposure (Fig. 9(b)). Furthermore, the HuA@ZIF-8 NPs did not appear to be cytotoxic during short exposure periods. Therefore, given the advantages of NIR-induced PTT, great antibacterial efficiency and biodegradability, this light-response platform is

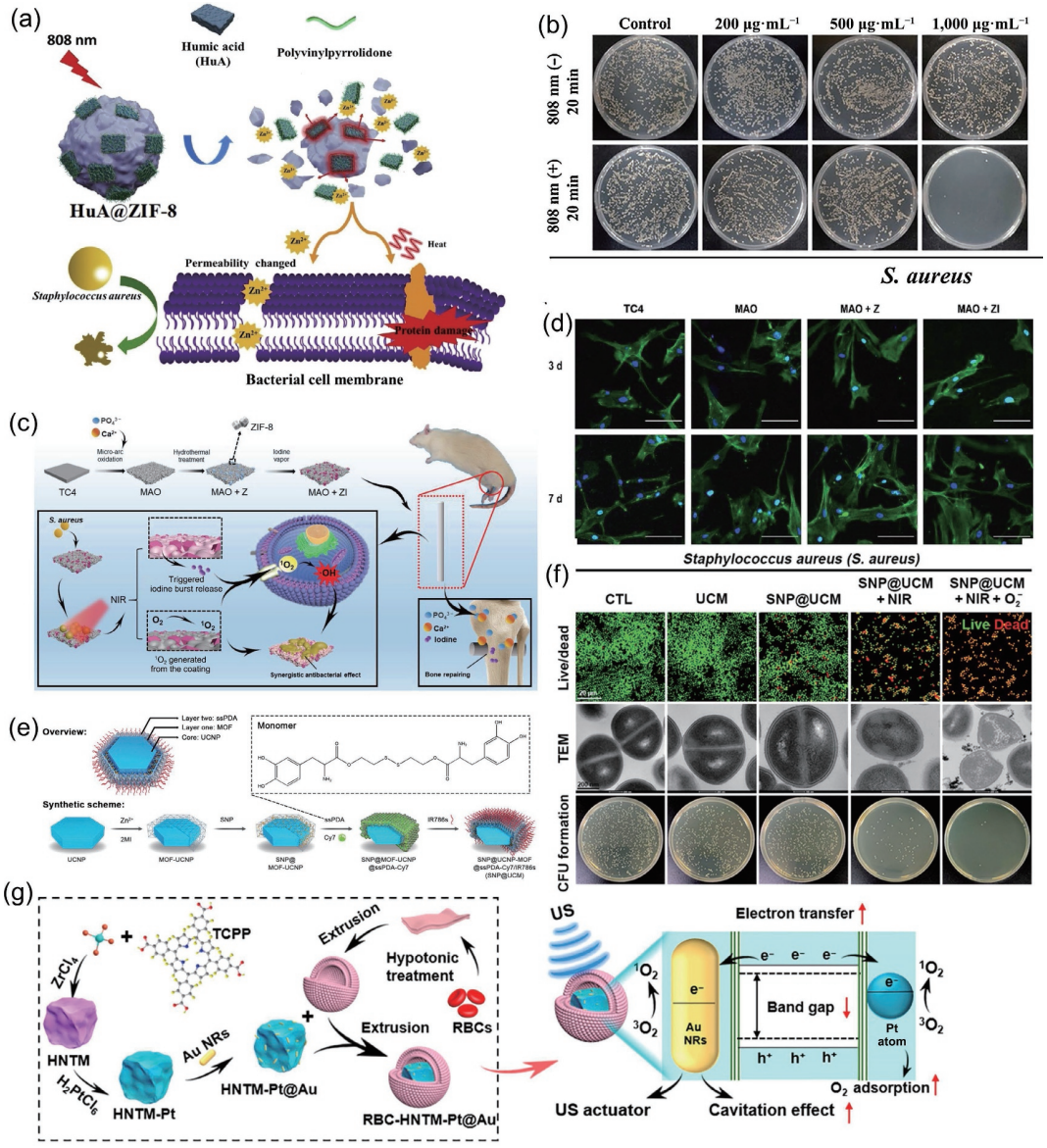

Figure 9 (a) Schematic of the sterilization on HuA@ZIF-8. (b) Typical photographs of viable colonies formed by *S. aureus* after treating the bacteria with or without 808 nm NIR laser irradiation for 20 min. (a) and (b) Reproduced with permission from Ref. [59], © Elsevier B. V. 2020. (c) Schematic illustration of the synthesis process, hierarchical structure of MAO + ZI coating system, the antibacterial process (*S. aureus*) guided by NIR. (d) Fluorescent images of the hBMSCs cultivated on different sheets for 3 and 7 days (Scale bar = 75 μm). (c) and (d) Reproduced with permission from Ref. [215], © Wiley-VCH GmbH 2021. (e) Schematic diagram of the synthesis of SNP@UCM. (f) Antibacterial activity of the indicated treatments against *S. aureus* as determined by bacterial live/dead staining, TEM analysis, and colony-forming unit (CFU) counts. (e) and (f) Reproduced with permission from Ref. [216], © Wiley-VCH GmbH 2021. (g) Synthesis of the RBC-HNTM-Pt@Au, mechanism, and the treatment of osteomyelitis. Reproduced with permission from Ref. [217], © American Chemical Society 2021.

promising for public health applications.

In fact, it is also a promising strategy to apply ZIF materials in conjunction with PTT for the treatment of implanted infections. Teng et al. [215] reported a synergistic system constructed by immobilizing ZIF-8 on micro arc oxidative (MAO) titanium surface, and then loaded iodine onto ZIF-8 coating. The nanocomposite substantially released iodine under NIR and activated ROS oxidative stress to enhance anti-*S. aureus* efficacy (Fig. 9(c)). Furthermore, the nuclei and actin protein of human mesenchymal stem cells from bone marrow (hBMSCs) showed normal morphology after MAO and MAO-ZI treatment, indicating that the composite not only exhibited good implant biocompatibility, but also supported osteogenic differentiation of bone marrow stromal cells (Fig. 9(d)).

Recently, a novel NIR-triggered NO nanogenerator (SNP@MOF-UCNP@ssPDA-Cy7/IR786s, abbreviated as SNP@UCM) was presented by Yang' group [216]. The nanomaterial was designed by using ZIF-8 layer loaded with sodium nitroprusside (SNP) as a coating and upconversion nanoparticle (UCNP) as the core of the nanogenerator. To avoid SNP leakage, a ROS response layer (ssPDA) was coated onto the surface to form the SNP@MOF-UCNP@ssPDA (Fig. 9(e)). As shown in Fig. 9(f), staining of live/dead bacteria showed that the number of bacteria significantly reduced after NIR irradiation combined with SNP@UCM treatment against *S. aureus*. Moreover, the obvious damage of bacterial membrane and DNA damage can be found in *S. aureus* observation.

9.3 SDT based on MOF materials

In 1989, Prof. Yumita firstly reported SDT, and then it evolved as a promising therapeutic approach for cancer and infectious disease treatment over recent decades [234]. The principle of SDT is that sonosensitizers are activated by low intensity ultrasound and produce ROS for the treatment of tumors and infectious diseases. SDT shows great potential in deep diseases by leveraging ultrasound's superior tissue penetration and non-invasiveness. In

the past decade, many research revealed highly efficient SDT with a variety of sound sensitizing agents, including curcumin [235, 236], Bengal rose [237], B hypochlorite [238], and some porphyrins [239, 240]. However, it was also found that some inherent limitations in SDT existed, such as poor tumor enrichment effect of small molecule acoustic sensitizer and low quantum yield of inorganic acoustic sensitizer. With the rapid development of nanotechnology, many new nanoplatforms have been applied to SDT. Specially, in recent years, some biocompatible MOF-based nanomaterials have been reasonably designed and shown great potential in sonodynamic therapy and catalytic nanomedicine [241, 242].

As shown in Fig. 9(g), Yu and co-workers [217] reported a multifunctional system for SDT, which was designed to the effective treatment of MRSA infection with osteomyelitis. Pt single-atom was first fixed on the zirconium-based porphyrin MOF (HNTM), and then used the Au NRs as US response actuators. Finally, in order to reduce the biological toxicity of the material, HNTM-Pt@Au was coated on the membrane of red blood cells (RBC) to synthesize RBC-HNTM-Pt@Au. Under US radiation, Pt atoms exhibited strong oxygen adsorption capacity and can produce toxic $^1O_2$. In addition, electron capture ability of Pt single atom and Au NRs was strong, Au NRs can also enhance US cavitation and improve the absorption of ultrasonic energy, thus increasing the production of $^1O_2$. The antibacterial activity test results showed that HNTM-Pt@Au showed a significant inhibitory effect on the growth of clinically isolated MRSA when activated by US. What's more, the authors further investigated the effect of RBC-HNTM-Pt@Au on osteomyelitis in MRSA-infected rats. Results showed that there was no ulceration at the surgical site in the US + 2-RBC-HNTM-Pt@Au group, indicating that the infection was significantly suppressed and the reduction in inflammatory response to bone loss was negligible.

10 Conclusions, challenges, and outlook

Due to the increased bacterial drug resistance, combating *S. aureus* infection is still a major challenge for clinicians and nursing professionals to address drug resistance. In the antibacterial field, developing effective, low toxicity, and environmentally friendly methods against bacteria is increasingly essential and imperative. MOF-based materials possess great potential in treating *S. aureus* infections due to their excellent porosity, tunable chemical constitute, open crystalline structure, and large surface area. Quite a few MOF-based nanocomposites have been reported for the controlled release of antimicrobial agents, including Cu, Zn, Ag, Fe-based MOF materials, etc., greatly expanding their antibacterial application. Various innovative biocatalytic strategies have been developed to prepare MOF-derivatives for treating bacterial infections. MOF-based materials also play an indispensable role in drug delivery and differentiation of antibiotics when it is used as a carrier. Furthermore, the energy excitation system can be constructed by regulating the component of MOF-based materials, which provides the potential value to combine PDT, PTT, and SCT for the treatment of bacterial infection. In term of antibiotics alternatives, high-efficient MOF-based antibiotics materials can obtain by rational designing, owing to their advantages of broad antibacterial spectrum, high efficiency, good stability, fast action time, and strong orientation. Except for the infectious diseases mentioned in this review, MOFs and MOF-based compounds also can treat other infectious caused by *S. aureus* including wound infection, catheter-associated urinary tract infections, and pulmonary tuberculosis. By these means, rational fabrication of MOF should be a feasible strategy for future development and application of antibacterial field. Although numerous efforts have been devoted to MOF-based materials, it still remains challenge to apply them in medical application.

Acceptable toxicology of substrate materials for antimicrobial applications. In the medical field represented by drug delivery and treatment, the human body can be directly exposed to pharmaceutical preparations containing artificial nanomaterials through injection, oral administration, and external application, which may accumulate in the liver and kidney rich in capillaries. Nanomaterials can also induce DNA damage, chromosomal aberration, and cell cycle disruption by directly interacting with DNA or chromosomes or by means of oxidative stress. The potential genotoxicity of nanoparticles depends on the size, shape, and surface modification. Thus, it is feasible to reduce the size of MOF-based nanomaterials, further relieving the accumulation in human organs, and more importantly allowing them to leave through metabolism.

Various biodegradable MOFs series also can be designed and developed due to their catalytic and biodegradable properties, endowing them a broad prospect to achieve biodegradable treatment of infectious diseases. With regard to MOFs, there are still some issues to be resolved such as poor combination with implants and unsatisfactory treatment of implant-related biofilm infections.

Achieving targeted drug delivery and precise release. The ideal drug carrier material must not only have clear structure, but also have regular shape, adjustable pore size, flexible drug load and can be prepared in large quantities. Most MOF-based systems show some degree of drug leakage during administration, resulting in a reduced drug release rate. In addition, the drug must reach the molecular target through multiple steps *in vivo*, such as enzyme degradation, gastrointestinal degradation, protein binding, and intracellular delivery. Thus, premature release of the drug from the carrier before reaching the target must be avoided. Although drug delivery during MOF synthesis can improve drug delivery efficiency, the process usually involves high pressure, high temperature, or toxic solvents. These rigorous synthesis conditions cause drug degradation, which seriously restricts the application of MOF as a bio-safe drug delivery system. Current examples mainly focused on reasonable surface modification, which is expected to reduce the leakage of active drugs and endow NPs active targeting capability.

Due to the easy decomposition of MOFs in physiological environments, the formation of stable MOFs structures is critical by introducing stable coordination bonds and intermolecular interactions such as hydrogen bonds. Even more to the point, computer simulations can be used to study antimicrobial loading and release of MOFs to predict pharmacokinetics.

How to target sterilization is a big challenge in practical application. At present, most of the MOF-based nanomaterials can be spectroscopically sterilized, but still exist a wide variety of bacteria. It is well known that there are normal colonizing bacteria and pathogenic bacteria in human body and on body surface. However, biological materials seem like "Blind God of War", regardless of good or bad, they can be caught in a net. Thus, the research on the antimicrobial activity of MOFs should not be limited to a few clinically isolated or traditional model strains and drug-resistant strains in food, but also should be expanded to explore a variety of pathogenic microorganisms in the biomedical field.

The bactericidal mechanism of MOF is still unclear. Although the detailed bactericidal mechanism of MOF has been comprehensively studied *in vitro*, physiological conditions are far more complex than experimental simulations. What's more, *in vitro* results could not really show the same results *in vivo* as well

as the lack of monitor methods of nanomaterials in body. With the development of characterization techniques, it is expected that more advanced detection strategies will help to gain insights on catalysis *in situ* physiological conditions.

In addition, it is not clear whether MOF material will cause bacterial resistance, and there is a lack of methods for monitoring drug resistance. Cyclic plate counting experiment can be used to monitor the bacterial resistance of MOF-based materials, but the mechanism of drug resistance is ambiguous. As for bactericidal MOF-based nanomaterials, transforming them into common clinical antibiotics is another major challenge. In future research, the range of potential toxicity and pathogenicity from ion leakage into the human body should all be taken into consideration. This needs propels that MOFs with single-atom metal catalytic centers appear to be a good candidate for clinical trials due to the high catalytic activity while avoiding ion leakage.

The synergistic sterilization of PDT, PTT, and SCT represents higher sterilization efficiency than the individual MOF material. However, considering practical and clinical applications, the relevant multifunctional platforms are hard to implement and always increase the cost. Therefore, future research on MOF-based material should be paid more attention to find the right balance between bactericidal performance and practical operability. In addition, the drawbacks of MOFs reduced their usefulness in many aspects such as production cost, biocompatibility, and toxicity, but MOFs are still expected to be rationalized in the future. In this rapidly developing new field, we are confident that these obstacles will be overcome in the future and that the use of MOF against bacteria will achieve significant advances in medicine.

References

[1] Mermel, L. A.; Cartony, J. M.; Covington, P.; Maxey, G.; Morse, D. Methicillin-resistant *Staphylococcus aureus* colonization at different body sites: A prospective, quantitative analysis. *J. Clin. Microbiol.* **2011**, *49*, 1119–1121.

[2] Blicharz, L.; Michalak, M.; Szymanek-Majchrzak, K.; Młynarczyk, G.; Skowroński, K.; Rudnicka, L.; Samochocki, Z. The propensity to form biofilm *in vitro* by *Staphylococcus aureus* strains isolated from the anterior nares of patients with atopic dermatitis: Clinical associations. *Dermatology* **2021**, *237*, 528–534.

[3] Von Eiff, C.; Becker, K.; Machka, K.; Stammer, H.; Peters, G. Nasal carriage as a source of *Staphylococcus aureus* bacteremia. *N. Engl. J. Med.* **2001**, *344*, 11–16.

[4] Sollid, J. U. E.; Furberg, A. S.; Hanssen, A. M.; Johannessen, M. *Staphylococcus aureus*: Determinants of human carriage. *Infect. Genet. Evol.* **2014**, *21*, 531–541.

[5] Tong, S. Y. C.; Davis, J. S.; Eichenberger, E.; Holland, T. L.; Fowler, V. G. Jr. *Staphylococcus aureus* infections: Epidemiology, pathophysiology, clinical manifestations, and management. *Clin. Microbiol. Rev.* **2015**, *28*, 603–661.

[6] Laupland, K. B. Incidence of bloodstream infection: A review of population-based studies. *Clin. Microbiol. Infect.* **2013**, *19*, 492–500.

[7] Sampedro, G. R.; DeDent, A. C.; Becker, R. E. N.; Berube, B. J.; Gebhardt, M. J.; Cao, H. Y.; Bubeck Wardenburg, J. Targeting *Staphylococcus aureus* α-toxin as a novel approach to reduce severity of recurrent skin and soft-tissue infections. *J. Infect. Dis.* **2014**, *210*, 1012–1018.

[8] Laxminarayan, R.; Duse, A.; Wattal, C.; Zaidi, A. K. M.; Wertheim, H. F. L.; Sumpradit, N.; Vlieghe, E.; Hara, G. L.; Gould, I. M.; Goossens, H. et al. Antibiotic resistance—The need for global solutions. *Lancet Infect. Dis.* **2013**, *13*, 1057–1098.

[9] Blair, J. M. A.; Webber, M. A.; Baylay, A. J.; Ogbolu, D. O.; Piddock, L. J. V. Molecular mechanisms of antibiotic resistance. *Nat. Rev. Microbiol.* **2015**, *13*, 42–51.

[10] Li, R.; Chen, T. T.; Pan, X. L. Metal-organic-framework-based materials for antimicrobial applications. *ACS Nano* **2021**, *15*, 3808–3848.

[11] Pettinari, C.; Pettinari, R.; Di Nicola, C.; Tombesi, A.; Scuri, S.; Marchetti, F. Antimicrobial MOFs. *Coord. Chem. Rev.* **2021**, *446*, 214121.

[12] Nong, W. Q.; Wu, J.; Ghiladi, R. A.; Guan, Y. G. The structural appeal of metal-organic frameworks in antimicrobial applications. *Coord. Chem. Rev.* **2021**, *442*, 214007.

[13] Gorai, T.; Schmitt, W.; Gunnlaugsson, T. Highlights of the development and application of luminescent lanthanide based coordination polymers, MOFs and functional nanomaterials. *Dalton Trans.* **2021**, *50*, 770–784.

[14] Sun, T. T.; Xu, L. B.; Wang, D. S.; Li, Y. D. Metal organic frameworks derived single atom catalysts for electrocatalytic energy conversion. *Nano Res.* **2019**, *12*, 2067–2080.

[15] Giliopoulos, D.; Zamboulis, A.; Giannakoudakis, D.; Bikiaris, D.; Triantafyllidis, K. Polymer/metal organic framework (MOF) nanocomposites for biomedical applications. *Molecules* **2020**, *25*, 185.

[16] Liu, Y. W.; Zhou, L. Y.; Dong, Y.; Wang, R.; Pan, Y.; Zhuang, S. Z.; Liu, D.; Liu, J. Q. Recent developments on MOF-based platforms for antibacterial therapy. *RSC Med. Chem.* **2021**, *12*, 915–928.

[17] Omidi, M. ; Firoozeh, F. ; Saffari, M. ; Sedaghat, H. ; Zibaei, M. ; Khaledi, A. Ability of biofilm production and molecular analysis of *spa* and *ica* genes among clinical isolates of methicillin-resistant *Staphylococcus aureus*. *BMC Res. Notes* **2020**, *13*, 19.

[18] Williams, R. E. O. Healthy carriage of *Staphylococcus aureus*: Its prevalence and importance. *Bacteriol. Rev.* **1963**, *27*, 56–71.

[19] Wertheim, H. F. L.; Melles, D. C.; Vos, M. C.; van Leeuwen, W.; van Belkum, A.; Verbrugh, H. A.; Nouwen, J. L. The role of nasal carriage in *Staphylococcus aureus* infections. *Lancet Infect. Dis.* **2005**, *5*, 751–762.

[20] Boyle-Vavra, S.; Daum, R. S. Community-acquired methicillinresistant *Staphylococcus aureus*: The role of Panton-Valentine leukocidin. *Lab. Invest.* **2007**, *87*, 3–9.

[21] Lowy, F. D. *Staphylococcus aureus* infections. *N. Engl. J. Med.* **1998**, *339*, 520–532.

[22] Archer, G. L. *Staphylococcus aureus*: A well-armed pathogen. *Clin. Infect. Dis.* **1998**, *26*, 1179–1181.

[23] Boyce, J. M.; Pittet, D. Guideline for hand hygiene in health-care settings. Recommendations of the healthcare infection control practices advisory committee and the HICPAC/SHEA/APIC/IDSA hand hygiene task force. Society for healthcare epidemiology of America/Association for professionals in infection control/infectious diseases society of America. *MMWR Recomm. Rep.* **2002**, *51*, 1–45.

[24] Sherertz, R. J.; Reagan, D. R.; Hampton, K. D.; Robertson, K. L.; Streed, S. A.; Hoen, H. M.; Thomas, R.; Gwaltney, J. M. Jr. A cloud adult: The *Staphylococcus aureus*–virus interaction revisited. *Ann. Intern. Med.* **1996**, *124*, 539–547.

[25] Zimmerli, W.; Sendi, P. Pathogenesis of implant-associated infection: The role of the host. *Semin. Immunopathol.* **2011**, *33*, 295–306.

[26] Foster, T. J. Immune evasion by staphylococci. *Nat. Rev. Microbiol.* **2005**, *3*, 948–958.

[27] Gladstone, G. P. Van Heyningen, W. E. Staphylococcal leucocidins. *Br. J. Exp. Pathol.* **1957**, *38*, 123–137.

[28] Grumann, D.; Nübel, U.; Bröker, B. M. *Staphylococcus aureus* toxins—Their functions and genetics. *Infect. Genet. Evol.* **2014**, *21*, 583–592.

[29] Ma, T. M. ; VanEpps, J. S. ; Solomon, M. J. Structure, mechanics, and instability of fibrin clot infected with *Staphylococcus epidermidis*. *Biophys. J.* **2017**, *113*, 2100–2109.

[30] Prestinaci, F.; Pezzotti, P.; Pantosti, A. Antimicrobial resistance: A global multifaceted phenomenon. *Pathog. Glob. Health* **2015**, *109*, 309–318.

[31] Manna, D. K.; Mandal, A. K.; Sen, I. K.; Maji, P. K.; Chakraborti, S.; Chakraborty, R.; Islam, S. S. Antibacterial and DNA degradation potential of silver nanoparticles synthesized via green route. *Int. J. Biol. Macromol.* **2015**, *80*, 455–459.

[32] Alabi, A. S.; Frielinghaus, L.; Kaba, H.; Kösters, K.; Huson, M. A. M.; Kahl, B. C.; Peters, G.; Grobusch, M. P.; Issifou, S.; Kremsner, P. G. et al. Retrospective analysis of antimicrobial resistance and bacterial spectrum of infection in Gabon, Central Africa. *BMC Infect. Dis.* **2013**, *13*, 455.

[33] Klein, E. Y.; Sun, L.; Smith, D. L.; Laxminarayan, R. The changing epidemiology of methicillin-resistant *Staphylococcus aureus* in the United States: A national observational study. *Am. J. Epidemiol.* **2013**, *177*, 666–674.

[34] Santajit, S.; Indrawattana, N. Mechanisms of antimicrobial resistance in ESKAPE pathogens. *BioMed Res. Int.* **2016**, *2016*, 2475067.

[35] Ansari, S.; Nepal, H. P.; Gautam, R.; Shrestha, S.; Chhetri, M. R.; Chapagain, M. L. *Staphylococcus Aureus*: Methicillin resistance and small colony variants from pyogenic infections of skin, soft tissue and bone. *J. Nepal Health Res. Counc.* **2015**, *13*, 126–132.

[36] Lakhundi, S.; Zhang, K. Y. Methicillin-resistant *Staphylococcus aureus*: Molecular characterization, evolution, and epidemiology. *Clin. Microbiol. Rev.* **2018**, *31*, e00020–18.

[37] Ansari, S.; Jha, R. K.; Mishra, S. K.; Tiwari, B. R.; Asaad, A. M. Recent advances in *Staphylococcus aureus* infection: Focus on vaccine development. *Infect. Drug Resist.* **2019**, *12*, 1243–1255.

[38] Johnson, N. B.; Hayes, L. D.; Brown, K.; Hoo, E. C.; Ethier, K. A. CDC national health report: Leading causes of morbidity and mortality and associated behavioral risk and protective factors United States, 2005–2013. *MMWR Suppl.* **2014**, *63*, 3–27.

[39] Jean, S. S.; Hsueh, P. R. High burden of antimicrobial resistance in Asia. *Int. J. Antimicrob. Agents* **2011**, *37*, 291–295.

[40] Wolk, D. M.; Struelens, M. J.; Pancholi, P.; Davis, T.; Della-Latta, P.; Fuller, D.; Picton, E.; Dickenson, R.; Denis, O.; Johnson, D. et al. Rapid detection of *Staphylococcus aureus* and methicillinresistant *S. aureus* (MRSA) in wound specimens and blood cultures: Multicenter preclinical evaluation of the Cepheid Xpert MRSA/SA skin and soft tissue and blood culture assays. *J. Clin. Microbiol.* **2009**, *47*, 823–826.

[41] Hurley, J. C. Risk of death from methicillin-resistant *Staphylococcus aureus* bacteraemia: A meta-analysis. *Med. J. Aust.* **2002**, *176*, 188.

[42] Fortuin-de Smidt, M. C.; Singh-Moodley, A.; Badat, R.; Quan, V.; Kularatne, R.; Nana, T.; Lekalakala, R.; Govender, N. P.; Perovic, O. *Staphylococcus aureus* bacteraemia in Gauteng academic hospitals, South Africa. *Int. J. Infect. Dis.* **2015**, *30*, 41–48.

[43] Zou, L. L.; Wang, J.; Gao, Y.; Ren, X. Y.; Rottenberg, M. E.; Lu, J.; Holmgren, A. Synergistic antibacterial activity of silver with antibiotics correlating with the upregulation of the ROS production. *Sci. Rep.* **2018**, *8*, 11131.

[44] Mohammed, Y. H. E.; Manukumar, H. M.; Rakesh, K. P.; Karthik, C. S.; Mallu, P.; Qin, H. L. Vision for medicine: *Staphylococcus aureus* biofilm war and unlocking key's for anti-biofilm drug development. *Microb. Pathog.* **2018**, *123*, 339–347.

[45] Yougbare, S.; Chang, T. K.; Tan, S. H.; Kuo, J. C.; Hsu, P. H.; Su, C. Y.; Kuo, T. R. Antimicrobial gold nanoclusters: Recent developments and future perspectives. *Int. J. Mol. Sci.* **2019**, *20*, 2924.

[46] Fletcher, S. Understanding the contribution of environmental factors in the spread of antimicrobial resistance. *Environ. Health Prev. Med.* **2015**, *20*, 243–252.

[47] Andersson, D. I.; Hughes, D. Kubicek-Sutherland, J. Z. Mechanisms and consequences of bacterial resistance to antimicrobial peptides. *Drug Resist. Updates* **2016**, *26*, 43–57.

[48] Archer, N. K.; Mazaitis, M. J.; Costerton, J. W.; Leid, J. G.; Powers, M. E.; Shirtliff, M. E. *Staphylococcus aureus* biofilms: Properties, regulation, and roles in human disease. *Virulence* **2011**, *2*, 445–459.

[49] Yaghi, O. M.; O'Keeffe, M.; Ockwig, N. W.; Chae, H. K.; Eddaoudi, M.; Kim, J. Reticular synthesis and the design of new materials. *Nature* **2003**, *423*, 705–714.

[50] Lee, J. Y.; Farha, O. K.; Roberts, J.; Scheidt, K. A.; Nguyen, S. B. T.; Hupp, J. T. Metal-organic framework materials as catalysts. *Chem. Soc. Rev.* **2009**, *38*, 1450–1459.

[51] Xue, Y. P.; Zhao, G. C.; Yang, R. Y.; Chu, F.; Chen, J.; Wang, L.; Huang, X. B. 2D metal-organic framework-based materials for electrocatalytic, photocatalytic and thermocatalytic applications. *Nanoscale* **2021**, *13*, 3911–3936.

[52] Shen, M. F.; Forghani, F.; Kong, X. Q.; Liu, D. D.; Ye, X. Q.; Chen, S. G.; Ding, T. Antibacterial applications of metal-organic frameworks and their composites. *Compr. Rev. Food Sci. Food Saf.* **2020**, *19*, 1397–1419.

[53] Usman, K. A. S.; Maina, J. W.; Seyedin, S.; Conato, M. T.; Payawan, L. M.; Dumée, L. F.; Razal, J. M. Downsizing metalorganic frameworks by bottom-up and top-down methods. *NPG Asia Mater.* **2020**, *12*, 58.

[54] Zhang, Y. M.; Zhang, X.; Song, J.; Jin, L. M.; Wang, X. T.; Quan, C. S. Ag/H-ZIF-8 nanocomposite as an effective antibacterial agent against pathogenic bacteria. *Nanomaterials* **2019**, *9*, 1579.

[55] Tippayawat, P.; Phromviyo, N.; Boueroy, P.; Chompoosor, A. Green synthesis of silver nanoparticles in aloe vera plant extract prepared by a hydrothermal method and their synergistic antibacterial activity. *PeerJ* **2016**, *4*, e2589.

[56] Wang, H.; Synatschke, C. V.; Raup, A.; Jérôme, V.; Freitag, R.; Agarwal, S. Oligomeric dual functional antibacterial polycaprolactone. *Polym. Chem.* **2014**, *5*, 2453–2460.

[57] Carović-Stanko, K. ; Orlić, S. ; Politeo, O. ; Strikić, F. ; Kolak, I. ; Milos, M. ; Satovic, Z. Composition and antibacterial activities of essential oils of seven *Ocimum taxa*. *Food Chem.* **2010**, *119*, 196–201.

[58] Mao, C. Y.; Xiang, Y. M.; Liu, X. M.; Cui, Z. D.; Yang, X. J.; Li, Z. Y.; Zhu, S. L.; Zheng, Y. F.; Yeung, K. W. K.; Wu, S. L. Repeatable photodynamic therapy with triggered signaling pathways of fibroblast cell proliferation and differentiation to promote bacteria-accompanied wound healing. *ACS Nano* **2018**, *12*, 1747–1759.

[59] Liu, Z. W.; Tan, L.; Liu, X. M.; Liang, Y. Q.; Zheng, Y. F.; Yeung, K. W. K.; Cui, Z. D.; Zhu, S. L.; Li, Z. Y.; Wu, S. L. Zn2+-assisted photothermal therapy for rapid bacteria-killing using biodegradable humic acid encapsulated MOFs. *Colloids Surf. B Biointerfaces* **2020**, *188*, 110781.

[60] Pang, X.; Xiao, Q. C.; Cheng, Y.; Ren, E.; Lian, L. L.; Zhang, Y.; Gao, H. Y.; Wang, X. Y.; Leung, W.; Chen, X. Y. et al. Bacteria responsive nanoliposomes as smart sonotheranostics for multidrug resistant bacterial infections. *ACS Nano* **2019**, *13*, 2427–2438.

[61] Zhang, L.; Liu, Z. W.; Deng, Q. Q.; Sang, Y. J.; Dong, K.; Ren, J. S.; Qu, X. G. Nature-inspired construction of MOF@COF nanozyme with active sites in tailored microenvironment and pseudopodia-like surface for enhanced bacterial inhibition. *Angew. Chem. Int. Ed.* **2021**, *60*, 3469–3474.

[62] Li, T.; Qiu, H. Q.; Liu, N.; Li, J. W.; Bao, Y. H.; Tong, W. J. Construction of self-activated cascade metal-organic framework/enzyme hybrid nanoreactors as antibacterial agents. *Colloids Surf. B Biointerfaces* **2020**, *191*, 111001.

[63] Lin, S.; Liu, X. M.; Tan, L.; Cui, Z. D.; Yang, X. J.; Yeung, K. W. K.; Pan, H. B.; Wu, S. L. Porous iron-carboxylate metal-organic framework: A novel bioplatform with sustained antibacterial efficacy and nontoxicity. *ACS Appl. Mater. Interfaces* **2017**, *9*, 19248–19257.

[64] Fan, X.; Yang, F.; Huang, J. B.; Yang, Y.; Nie, C. X.; Zhao, W. F.; Ma, L.; Cheng, C.; Zhao, C. S.; Haag, R. Metal-organic-framework derived 2D carbon nanosheets for localized multiple bacterial eradication and augmented anti-infective therapy. *Nano Lett.* **2019**, *19*, 5885–5896.

[65] Luo, Y.; Li, J.; Liu, X. M.; Tan, L.; Cui, Z. D.; Feng, X. B.; Yang, X. J.; Liang, Y. Q.; Li, Z. Y.; Zhu, S. L. et al. Dual metal-organic framework heterointerface. *ACS Cent. Sci.* **2019**, *5*, 1591–1601.

[66] Ge, C. C.; Wu, R. F.; Chong, Y.; Fang, G.; Jiang, X. M.; Pan, Y.; Chen, C. Y.; Yin, J. J. Synthesis of Pt hollow nano dendrites with enhanced peroxidase-like activity against bacterial infections: Implication for wound healing. *Adv. Funct. Mater.* **2018**, *28*, 1801484.

[67] Zirak Hassan Kiadeh, S.; Ghaee, A.; Farokhi, M.; Nourmohammadi, J.; Bahi, A.; Ko, F. K. Electrospun pectin/modified copper-based metal-organic framework (MOF) nanofibers as a drug delivery system. *Int. J. Biol. Macromol.* **2021**,

173, 351–365.
[68] Xiang, Y. M.; Mao, C. Y.; Liu, X. M.; Cui, Z. D.; Jing, D. D.; Yang, X. J.; Liang, Y. Q.; Li, Z. Y.; Zhu, S. L.; Zheng, Y. F. et al. Rapid and superior bacteria killing of carbon quantum dots/ZnO decorated injectable folic acid-conjugated PDA hydrogel through dual-light triggered ROS and membrane permeability. *Small* **2019**, *15*, 1900322.
[69] Geveke, D. J.; Gurtler, J.; Zrang, H. Q. Inactivation of *Lactobacillus plantarum* in apple cider, using radio frequency electric fields. *J. Food. Prot.* **2009**, *72*, 656–661.
[70] Donlan, R. M.; Costerton, J. W. Biofilms: Survival mechanisms of clinically relevant microorganisms. *Clin. Microbiol. Rev.* **2002**, *15*, 167–193.
[71] Liu, Z. W.; Wang, F. M.; Ren, J. S.; Qu, X. G. A series of MOF/Cebased nanozymes with dual enzyme-like activity disrupting biofilms and hindering recolonization of bacteria. *Biomaterials* **2019**, *208*, 21–31.
[72] Haas, K. L.; Franz, K. J. Application of metal coordination chemistry to explore and manipulate cell biology. *Chem. Rev.* **2009**, *109*, 4921–4960.
[73] Ma, Z.; Jacobsen, F. E.; Giedroc, D. P. Coordination chemistry of bacterial metal transport and sensing. *Chem. Rev.* **2009**, *109*, 4644–4681.
[74] Pearson, R. G. Hard and soft acids and bases—The evolution of a chemical concept. *Coord. Chem. Rev.* **1990**, *100*, 403–425.
[75] Nies, D. H. Efflux-mediated heavy metal resistance in prokaryotes. *FEMS Microbiol. Rev.* **2003**, *27*, 313–339.
[76] Harrison, J. J.; Ceri, H.; Turner, R. J. Multimetal resistance and tolerance in microbial biofilms. *Nat. Rev. Microbiol.* **2007**, *5*, 928–938.
[77] Howarth, A. J.; Liu, Y. Y.; Li, P.; Li, Z. Y.; Wang, T. C.; Hupp, J. T.; Farha, O. K. Chemical, thermal and mechanical stabilities of metal-organic frameworks. *Nat. Rev. Mater.* **2016**, *1*, 15018.
[78] Feng, M. B.; Zhang, P.; Zhou, H. C.; Sharma, V. K. Water-stable metal-organic frameworks for aqueous removal of heavy metals and radionuclides: A review. *Chemosphere* **2018**, *209*, 783–800.
[79] Gordon, O.; Slenters, T. V.; Brunetto, P. S.; Villaruz, A. E.; Sturdevant, D. E.; Otto, M.; Landmann, R.; Fromm, K. M. Silver coordination polymers for prevention of implant infection: Thiol interaction, impact on respiratory chain enzymes, and hydroxyl radical induction. *Antimicrob. Agents Chemother.* **2010**, *54*, 4208–4218.
[80] Lemire, J. A.; Harrison, J. J.; Turner, R. J. Antimicrobial activity of metals: Mechanisms, molecular targets and applications. *Nat. Rev. Microbiol.* **2013**, *11*, 371–384.
[81] Medina, E. ; Pieper, D. H. Tackling threats and future problems of multidrug-resistant bacteria. In *How to Overcome the Antibiotic Crisis: Facts*, *Challenges*, *Technologies and Future Perspectives*, Cham, 2016, pp 3–33.
[82] Singh, S. B.; Barrett, J. F. Empirical antibacterial drug discovery foundation in natural products. *Biochem. Pharmacol.* **2006**, *71*, 1006–1015.
[83] Fasnacht, M.; Polacek, N. Oxidative stress in bacteria and the central dogma of molecular biology. *Front. Mol. Biosci.* **2021**, *8*, 671037.
[84] West, J. D.; Marnett, L. J. Endogenous reactive intermediates as modulators of cell signaling and cell death. *Chem. Res. Toxicol.* **2006**, *19*, 173–194.
[85] Van Acker, H.; Coenye, T. The role of reactive oxygen species in antibiotic-mediated killing of bacteria. *Trends Microbiol.* **2017**, *25*, 456–466.
[86] Kiley, P. J.; Beinert, H. The role of Fe-S proteins in sensing and regulation in bacteria. *Curr. Opin. Microbiol.* **2003**, *6*, 181–185.
[87] Soltani, S.; Akhbari, K. Cu-BTC metal-organic framework as a biocompatible nanoporous carrier for chlorhexidine antibacterial agent. *J. Biol. Inorg. Chem* **2022**, *27*, 81–81.
[88] Yu, P. L.; Han, Y. J.; Han, D. L.; Liu, X. M.; Liang, Y. Q.; Li, Z. Y.; Zhu, S. L.; Wu, S. L. *In-situ* sulfuration of Cu-based metalorganic framework for rapid near-infrared light sterilization. *J. Hazard. Mater.* **2020**, 390.
[89] Ren, X. Y.; Yang, C. Y.; Zhang, L.; Li, S. H.; Shi, S.; Wang, R.; Zhang, X.; Yue, T. L.; Sun, J.; Wang, J. L. Copper metal-organic frameworks loaded on chitosan film for the efficient inhibition of bacteria and local infection therapy. *Nanoscale* **2019**, *11*, 11830–11838.
[90] Wang, H. T.; Ao, D.; Lu, M. C.; Chang, N. Alteration of the morphology of polyvinylidene fluoride membrane by incorporating MOF-199 nanomaterials for improving water permeation with antifouling and antibacterial property. *J. Chin. Chem. Soc.* **2020**, *67*, 1807–1817.
[91] Singbumrung, K.; Motina, K.; Pisitsak, P.; Chitichotpanya, P.; Wongkasemjit, S.; Inprasit, T. Preparation of Cu-BTC/PVA fibers with antibacterial applications. *Fibers Polym.* **2018**, *19*, 1373–1378.
[92] Wang, S. Y.; Yan, F.; Ren, P.; Li, Y.; Wu, Q.; Fang, X. D.; Chen, F. F.; Wang, C. Incorporation of metal-organic frameworks into electrospun chitosan/poly (vinyl alcohol) nanofibrous membrane with enhanced antibacterial activity for wound dressing application. *Int. J. Biol. Macromol.* **2020**, *158*, 9–17.
[93] Tang, S. L. ; Zhang, L. L. ; Mao, X. Y. ; Shao, Y. L. ; Cao, M. G. ; Zhang, L. ; Liang, X. M. Pullulan-based nanocomposite films with enhanced hydrophobicity and antibacterial performances. *Polym. Bull.* , in press,https://doi.org/ 10.1007/s00289-021-03996-0.
[94] Gizer, S. G.; Sahiner, N. The effect of sulphur on the antibacterial properties of succinic acid-Cu(II) and mercaptosuccinic acid-Cu(II) MOFs. *Inorg. Chim. Acta* **2021**, *528*, 120611.
[95] Han, D. L.; Han, Y. J.; Li, J.; Liu, X. M.; Yeung, K. W. K.; Zheng, Y. F.; Cui, Z. D.; Yang, X. J.; Liang, Y. Q.; Li, Z. Y. et al. Enhanced photocatalytic activity and photothermal effects of Cu doped metal-organic frameworks for rapid treatment of bacteria infected wounds. *Appl. Catal. B-Environ.* **2020**, *261*, 118248.
[96] Liu, X. P.; Yan, Z. Q.; Zhang, Y.; Liu, Z. W.; Sun, Y. H.; Ren, J. S.; Qu, X. G. Two-dimensional metal-organic framework/enzyme hybrid nanocatalyst as a benign and self-activated cascade reagent for *in vivo* wound healing. *ACS Nano* **2019**, *13*, 5222–5230.
[97] Allahbakhsh, A.; Jarrahi, Z.; Farzi, G.; Shavandi, A. Three dimensional nanoporous Cu-BTC/graphene oxide nanocomposites with engineered antibacterial properties synthesized via a one-pot solvosonication process. *Mater. Chem. Phys.* **2022**, *277*, 125502.
[98] Wang, Z. Y. ; Guo, W. ; Zhang, K. ; Ye, Y. M. ; Wang, Y. M. ; Sui, D. ; Zhao, N. N. ; Xu, F. J. Two-dimensional copper metal-organic frameworks as antibacterial agents for biofilm treatment. *Sci. ChinaTechnol. Sci.* , in press,DOI: 10.1007/s11431-021-1963-3.
[99] Gwon, K.; Kim, Y.; Cho, H.; Lee, S.; Yang, S. H.; Kim, S. J.; Lee, D. N. Robust copper metal-organic framework-embedded polysiloxanes for biomedical applications: Its antibacterial effects on MRSA and *in vitro* cytotoxicity. *Nanomaterials* **2021**, *11*, 719.
[100] Azizabadi, O.; Akbarzadeh, F.; Danshina, S.; Chauhan, N. P. S. Sargazi, G. An efficient ultrasonic assisted reverse micelle synthesis route for Fe3O4@Cu-MOF/core–shell nanostructures and its antibacterial activities. *J. Solid State Chem.* **2021**, *294*, 121897.
[101] Can, M.; Demirci, S.; Sunol, A. K.; Sahiner, N. An amino acid, Lglutamic acid-based metal-organic frameworks and their antibacterial, blood compatibility, biocompatibility, and sensor properties. *Microporous Mesoporous Mater.* **2020**, *309*, 110533.
[102] Liu, Z.; Ye, J. W.; Rauf, A.; Zhang, S. Q.; Wang, G. Y.; Shi, S. Q.; Ning, G. L. A flexible fibrous membrane based on copper(II) metalorganic framework/poly(lactic acid) composites with superior antibacterial performance. *Biomater. Sci.* **2021**, *9*, 3851–3859.
[103] Bhardwaj, N.; Pandey, S. K.; Mehta, J.; Bhardwaj, S. K.; Kim, K. H.; Deep, A. Bioactive nano-metal-organic frameworks as antimicrobials against Gram-positive and Gram-negative bacteria. *Toxicol. Res.* **2018**, *7*, 931–941.
[104] Restrepo, J.; Serroukh, Z.; Santiago-Morales, J.; Aguado, S.; Gómez-Sal, P.; Mosquera, M. E. G.; Rosal, R. An antibacterial ZnMOF with hydrazinebenzoate linkers. *Eur. J. Inorg. Chem.* **2017**, *2017*, 574–580.
[105] Tamames-Tabar, C.; Imbuluzqueta, E.; Guillou, N.; Serre, C.; Miller, S. R.; Elkaïm, E.; Horcajada, P.; Blanco-Prieto, M. J. A Zn azelate MOF: Combining antibacterial effect. *Crystengcomm* **2015**, *17*, 456–462.

[106] Yang, Y.; Wu, X. Z.; He, C.; Huang, J. B.; Yin, S. Q.; Zhou, M.; Ma, L.; Zhao, W. F.; Qiu, L.; Cheng, C. et al. Metal-organic framework/Ag-based hybrid nanoagents for rapid and synergistic bacterial eradication. *ACS Appl. Mater. Interfaces* **2020**, *12*, 13698–13708.

[107] Ahmed, S. A.; Bagchi, D.; Katouah, H. A.; Hasan, M. N.; Altass, H. M.; Pal, S. K. Enhanced water stability and photoresponsivity in metal-organic Framework (MOF): A potential tool to combat drug resistant bacteria. *Sci. Rep.* **2019**, *9*, 19372.

[108] Ahmad, N.; Samavati, A.; Nordin, N. A. H. M.; Jaafar, J.; Ismail, A. F.; Malek, N. A. N. N. Enhanced performance and antibacterial properties of amine-functionalized ZIF-8-decorated GO for ultrafiltration membrane. *Sep. Purif. Technol.* **2020**, *239*, 116554.

[109] Sacourbaravi, R.; Ansari-Asl, Z.; Kooti, M.; Nobakht, V.; Darabpour, E. Fabrication of Ag NPs/Zn-MOF nanocomposites and their application as antibacterial agents. *J. Inorg. Organomet. Polym. Mater.* **2020**, *30*, 4615–4621.

[110] Balasamy, R. J.; Ravinayagam, V.; Alomari, M.; Ansari, M. A.; Almofty, S. A.; Rehman, S.; Dafalla, H.; Marimuthu, P. R.; Akhtar, S.; Al Hamad, M. Cisplatin delivery, anticancer and antibacterial properties of Fe/SBA-16/ZIF-8 nanocomposite. *RSC Adv.* **2019**, *9*, 42395–42408.

[111] Chen, X. Y.; Ji, P. A microporous Zn(II)-MOF for solvent-free cyanosilylation and treatment effect against bacterial infection on burn patients via inhibiting the *Staphylococcus aureus* biofilm formation. *J. Inorg. Organomet. Polym. Mater.* **2021**, *31*, 492–499.

[112] Nakhaei, M.; Akhbari, K.; Kalati, M.; Phuruangrat, A. Antibacterial activity of three zinc-terephthalate MOFs and its relation to their structural features. *Inorg. Chim. Acta* **2021**, 522.

[113] Hao, Q. Q.; Cheng, L.; Dong, Z. Two Zn(II)-organic frameworks: Catalytic knoevenagel condensation and treatment activity on spine surgery incision infection via inhibiting *Staphylococcus aureus* biofilms formation. *J. Exp. Nanosci.* **2021**, *16*, 31–42.

[114] Dutta, B.; Pal, K.; Jana, K.; Sinha, C.; Mir, M. H. Fabrication of a Zn(II)-based 2D pillar bilayer metal-organic framework for antimicrobial activity. *Chemistryselect* **2019**, *4*, 9947–9951.

[115] Hu, Y. C.; Yang, H.; Wang, R. H.; Duan, M. L. Fabricating Ag@MOF-5 nanoplates by the template of MOF-5 and evaluating its antibacterial activity. *Colloids Surf. A:Physicochem. Eng. Aspects* **2021**, *626*, 127093.

[116] Xie, B. P.; Chai, J. W.; Fan, C.; Ouyang, J. H.; Duan, W. J.; Sun, B.; Chen, J.; Yuan, L. X.; Xu, X. Q.; Chen, J. X. Water-stable silver based metal-organic frameworks of quaternized carboxylates and their antimicrobial activity. *ACS Appl. Bio Mater.* **2020**, *3*, 8525–8531.

[117] Huang, X. J.; Yu, S. J.; Lin, W. X.; Yao, X.; Zhang, M. Y.; He, Q.; Fu, F. Y.; Zhu, H. L.; Chen, J. J. A metal-organic framework MIL-53(Fe) containing sliver ions with antibacterial property. *J. Solid State Chem.* **2021**, *302*, 122442.

[118] Arenas-Vivo, A.; Amariei, G.; Aguado, S.; Rosal, R.; Horcajada, P. An Ag-loaded photoactive nano-metal organic framework as a promising biofilm treatment. *Acta Biomater.* **2019**, *97*, 490–500.

[119] Zhang, M.; Wang, G. H.; Wang, D.; Zheng, Y. Q.; Li, Y. X.; Meng, W. Q.; Zhang, X.; Du, F. F.; Lee, S. Ag@MOF-loaded chitosan nanoparticle and polyvinyl alcohol/sodium alginate/chitosan bilayer dressing for wound healing applications. *Int. J. Biol. Macromol.* **2021**, *175*, 481–494.

[120] Huang, R. ; Cai, G. Q. ; Li, J. ; Li, X. S. ; Liu, H. T. ; Shang, X. L. ; Zhou, J. D. ; Nie, X. M. ; Gui, R. Platelet membrane-camouflaged silver metal-organic framework drug system against infections caused by methicillin-resistant *Staphylococcus aureus*. *J. Nanobiotechnol*. **2021**, *19*, 229.

[121] Hajibabaei, M.; Zendehdel, R.; Panjali, Z. Imidazole-functionalized Ag/MOFs as promising scaffolds for proper antibacterial activity and toxicity reduction of Ag nanoparticles. *J. Inorg. Organomet. P* **2020**, *30*, 4622–4626.

[122] Lu, X. Y.; Ye, J. W.; Zhang, D. K.; Xie, R. X.; Bogale, R. F.; Sun, Y.; Zhao, L. M.; Zhao, Q.; Ning, G. L. Silver carboxylate metalorganic frameworks with highly antibacterial activity and biocompatibility. *J. Inorg. Biochem.* **2014**, *138*, 114–121.

[123] Jaros, S. W.; da Silva, M. F. C. G.; Florek, M.; Oliveira, M. C.; Smoleński, P.; Pombeiro, A. J. L. Kirillov, A. M. Aliphatic dicarboxylate directed assembly of silver(I) 1, 3, 5-triaza-7-phosphaadamantane coordination networks: Topological versatility and antimicrobial activity. *Cryst. Growth Des.* **2014**, *14*, 5408–5417.

[124] Zirehpour, A.; Rahimpour, A.; Shamsabadi, A. A.; Sharifian, G. M.; Soroush, M. Mitigation of thin-film composite membrane biofouling via immobilizing nano-sized biocidal reservoirs in the membrane active layer. *Environ. Sci. Technol.* **2017**, *51*, 5511–5522.

[125] Seyedpour, S. F.; Firouzjaei, M. D.; Rahimpour, A.; Zolghadr, E.; Shamsabadi, A. A.; Das, P.; Afkhami, F. A.; Sadrzadeh, M.; Tiraferri, A.; Elliott, M. Toward sustainable tackling of biofouling implications and improved performance of TFC FO membranes modified by Ag-MOF nanorods. *ACS Appl. Mater. Interfaces* **2020**, *12*, 38285–38298.

[126] Fan, X.; Yang, F.; Nie, C. X.; Yang, Y.; Ji, H. F.; He, C.; Cheng, C.; Zhao, C. S. Mussel-inspired synthesis of NIR-responsive and biocompatible Ag-graphene 2D nanoagents for versatile bacterial disinfections. *ACS Appl. Mater. Interfaces* **2018**, *10*, 296–307.

[127] Yang, Y.; Ma, L.; Cheng, C.; Deng, Y. Y.; Huang, J. B.; Fan, X.; Nie, C. X.; Zhao, W. F.; Zhao, C. S. Nonchemotherapic and robust dual-responsive nanoagents with on-demand bacterial trapping, ablation, and release for efficient wound disinfection. *Adv. Funct. Mater.* **2018**, *28*, 1705708.

[128] D'Agostino, A.; Taglietti, A.; Desando, R.; Bini, M.; Patrini, M.; Dacarro, G.; Cucca, L.; Pallavicini, P.; Grisoli, P. Bulk surfaces coated with triangular silver nanoplates: Antibacterial action based on silver release and photo-thermal effect. *Nanomaterials* **2017**, *7*, 7.

[129] Zhang, C.; Hu, D. F.; Xu, J. W.; Ma, M. Q.; Xing, H. B.; Yao, K.; Ji, J.; Xu, Z. K. Polyphenol-assisted exfoliation of transition metal dichalcogenides into nanosheets as photothermal nanocarriers for enhanced antibiofilm activity. *ACS Nano* **2018**, *12*, 12347–12356.

[130] Li, Y. T.; Jin, J.; Wang, D. W.; Lv, J. W.; Hou, K.; Liu, Y. L.; Chen, C. Y.; Tang, Z. Y. Coordination-responsive drug release inside gold nanorod@metal-organic framework core–shell nanostructures for near-infrared-induced synergistic chemophotothermal therapy. *Nano Res.* **2018**, *11*, 3294–3305.

[131] Leighton, T. G.; Pickworth, M. J. W.; Walton, A. J.; Dendy, P. P. Studies of the cavitational effects of clinical ultrasound by sonoluminescence: 1. Correlation of sonoluminescence with the standing wave pattern in an acoustic field produced by a therapeutic unit. *Phys. Med. Biol.* **1988**, *33*, 1239–1248.

[132] Pan, X. T.; Wang, H. Y.; Wang, S. H.; Sun, X.; Wang, L. J.; Wang, W. W.; Shen, H. Y.; Liu, H. Y. Sonodynamic therapy (SDT): A novel strategy for cancer nanotheranostics. *Sci. China Life Sci.* **2018**, *61*, 415–426.

[133] Pan, X. T.; Bai, L. X.; Wang, H.; Wu, Q. Y.; Wang, H. Y.; Liu, S.; Xu, B. L.; Shi, X. H.; Liu, H. Y. Metal-organic-framework-derived carbon nanostructure augmented sonodynamic cancer therapy. *Adv. Mater.* **2018**, *30*, 1800180.

[134] Karimi Alavijeh, R.; Beheshti, S.; Akhbari, K.; Morsali, A. Investigation of reasons for metal-organic framework's antibacterial activities. *Polyhedron* **2018**, *156*, 257–278.

[135] Huxford, R. C.; Della Rocca, J.; Lin, W. B. Metal-organic frameworks as potential drug carriers. *Curr. Opin. Chem. Biol.* **2010**, *14*, 262–268.

[136] Yang, Q. H.; Xu, Q.; Jiang, H. L. Metal-organic frameworks meet metal nanoparticles: Synergistic effect for enhanced catalysis. *Chem. Soc. Rev.* **2017**, *46*, 4774–4808.

[137] Liang, S.; Wu, X. L.; Xiong, J.; Zong, M. H.; Lou, W. Y. Metalorganic frameworks as novel matrices for efficient enzyme immobilization: An update review. *Coord. Chem. Rev.* **2020**, *406*, 213149.

[138] McGuire, C. V.; Forgan, R. S. The surface chemistry of metalorganic frameworks. *Chem. Commun.* **2015**, *51*, 5199–5217.

[139] Kitagawa, S.; Furukawa, S. Porous coordination polymers having guest accessible functional organic sites. *Acta Cryst.* **2008**, *A64*, C104.

[140] Miller, S. R.; Heurtaux, D.; Baati, T.; Horcajada, P.; Grenèche, J.

M.; Serre, C. Biodegradable therapeutic MOFs for the delivery of bioactive molecules. *Chem. Commun.* **2010**, *46*, 4526–4528.
[141] Xing, L.; Cao, Y. Y.; Che, S. A. Synthesis of core–shell coordination polymernanoparticles (CPNs) for pH-responsive controlled drug release. *Chem. Commun.* **2012**, *48*, 5995–5997.
[142] Lashkari, E.; Wang, H.; Liu, L. S.; Li, J.; Yam, K. Innovative application of metal-organic frameworks for encapsulation and controlled release of allyl isothiocyanate. *Food Chem.* **2017**, *221*, 926–935.
[143] Kornblatt, A. P.; Nicoletti, V. G.; Travaglia, A. The neglected role of copper ions in wound healing. *J. Inorg. Biochem.* **2016**, *161*, 1–8.
[144] Mallick, S.; Sharma, S.; Banerjee, M.; Ghosh, S. S.; Chattopadhyay, A.; Paul, A. Iodine-stabilized Cu nanoparticle chitosan composite for antibacterial applications. *ACS Appl. Mater. Interfaces* **2012**, *4*, 1313–1323.
[145] Chen, S.; Tang, F.; Tang, L. Z.; Li, L. D. Synthesis of Cu nanoparticle hydrogel with self-healing and photothermal properties. *ACS Appl. Mater. Interfaces* **2017**, *9*, 20895–20903.
[146] Shams, S. ; Ahmad, W. ; Memon, A. H. ; Shams, S. ; Wei, Y. ; Yuan, Q. P. ; Liang, H. Cu/H3BTC MOF as a potential antibacterial therapeutic agent against *Staphylococcus aureus* and *Escherichia coli*. *New J. Chem*. **2020**, *44*, 17671–17678.
[147] Chui, S. S. Y. ; Lo, S. M. F. ; Charmant, J. P. H. ; Orpen, A. G. ; Williams, I. D. A chemically functionalizable nanoporous material [Cu3(TMA)2(H2O)3]*n*. *Science* **1999**, *283*, 1148–1150.
[148] Abbasi, A. R.; Akhbari, K.; Morsali, A. Dense coating of surface mounted CuBTC metal-organic framework nanostructures on silk fibers, prepared by layer-by-layer method under ultrasound irradiation with antibacterial activity. *Ultrason. Sonochem.* **2012**, *19*, 846–852.
[149] Zhang, S. Q.; Ye, J. W.; Sun, Y.; Kang, J.; Liu, J. H.; Wang, Y.; Li, Y. C.; Zhang, L. H.; Ning, G. L. Electrospun fibrous mat based on silver(I) metal-organic frameworks-polylactic acid for bacterial killing and antibiotic-free wound dressing. *Chem. Eng. J.* **2020**, *390*, 124523.
[150] da Silv Pinto, M.; Sierra-Avila, C. A.; Hinestroza, J. P. *In situ* synthesis of a Cu-BTC metal-organic framework (MOF 199) onto cellulosic fibrous substrates: Cotton. *Cellulose* **2012**, *19*, 1771–1779.
[151] Emam, H. E.; Darwesh, O. M.; Abdelhameed, R. M. In-growth metal organic framework/synthetic hybrids as antimicrobial fabrics and its toxicity. *Colloids Surf. B Biointerfaces* **2018**, *165*, 219–228.
[152] Kohsari, I.; Shariatinia, Z.; Pourmortazavi, S. M. Antibacterial electrospun chitosan-polyethylene oxide nanocomposite mats containing ZIF-8 nanoparticles. *Int. J. Biol. Macromol.* **2016**, *91*, 778–788.
[153] Mohanta, G. C.; Pandey, S. K.; Maurya, I. K.; Sahota, T. S.; Mondal, S. K.; Deep, A. Synergistic antimicrobial activity in ampicillin loaded core–shell ZnO@ZIF-8 Particles. *ChemistrySelect* **2019**, *4*, 12002–12009.
[154] Tao, B. L.; Zhao, W. K.; Lin, C. C.; Yuan, Z.; He, Y.; Lu, L.; Chen, M. W.; Ding, Y.; Yang, Y. L.; Xia, Z. Z. L. et al. Surface modification of titanium implants by ZIF-8@Levo/LBL coating for inhibition of bacterial-associated infection and enhancement of *in vivo* osseointegration. *Chem. Eng. J.* **2020**, *390*, 124621.
[155] Fan, X.; Yang, F.; Nie, C. X.; Ma, L.; Cheng, C.; Haag, R. Biocatalytic nanomaterials: A new pathway for bacterial disinfection. *Adv. Mater.* **2021**, *33*, 2100637.
[156] Rubin, H. N.; Neufeld, B. H.; Reynolds, M. M. Surface-anchored metal-organic framework-cotton material for tunable antibacterial copper delivery. *ACS Appl. Mater. Interfaces* **2018**, *10*, 15189–15199.
[157] Peng, C.; Kuai, Z. Y.; Zeng, T. Q.; Yu, Y.; Li, Z. F.; Zuo, J. T.; Chen, S.; Pan, S. J.; Li, L. WO3 nanorods/MXene composite as high performance electrode for supercapacitors. *J. Alloys Compd.* **2019**, *810*, 151928.
[158] Abednejad, A.; Ghaee, A.; Nourmohammadi, J.; Mehrizi, A. A. Hyaluronic acid/carboxylated zeolitic imidazolate framework film with improved mechanical and antibacterial properties. *Carbohydr. Polym.* **2019**, *222*, 115033.
[159] Liang, K.; Ricco, R.; Doherty, C. M.; Styles, M. J.; Bell, S.; Kirby, N.; Mudie, S.; Haylock, D.; Hill, A. J.; Doonan, C. J. et al. Biomimetic mineralization of metal-organic frameworks as protective coatings for biomacromolecules. *Nat. Commun.* **2015**, *6*, 7240.
[160] Li, S. X.; Wang, K. K.; Shi, Y. J.; Cui, Y. N.; Chen, B. L.; He, B.; Dai, W. B.; Zhang, H.; Wang, X. Q.; Zhong, C. L. et al. Novel biological functions of ZIF-NP as a delivery vehicle: High pulmonary accumulation, favorable biocompatibility, and improved therapeutic outcome. *Adv. Funct. Mater.* **2016**, *26*, 2715–2727.
[161] Huang, X. C.; Lin, Y. Y.; Zhang, J. P.; Chen, X. M. Ligand directed strategy for zeolite-type metal-organic frameworks: Zinc(II) imidazolates with unusual zeolitic topologies. *Angew. Chem. , Int. Ed.* **2006**, *45*, 1557–1559.
[162] Esfahanian, M.; Ghasemzadeh, M. A.; Razavian, S. M. H. Synthesis, identification and application of the novel metal-organic framework Fe3O4@PAA@ZIF-8 for the drug delivery of ciprofloxacin and investigation of antibacterial activity. *Artif. Cells Nanomed. Biotechnol.* **2019**, *47*, 2024–2030.
[163] Bradshaw, D.; Garai, A.; Huo, J. Metal-organic framework growth at functional interfaces: Thin films and composites for diverse applications. *Chem. Soc. Rev.* **2012**, *41*, 2344–2381.
[164] Tejero, R.; Anitua, E.; Orive, G. Toward the biomimetic implant surface: Biopolymers on titanium-based implants for bone regeneration. *Prog. Polym. Sci.* **2014**, *39*, 1406–1447.
[165] Tan, L.; Li, J.; Liu, X. M.; Cui, Z. D.; Yang, X. J.; Zhu, S. L.; Li, Z. Y.; Yuan, X. B.; Zheng, Y. F.; Yeung, K. W. K. et al. Rapid biofilm eradication on bone implants using red phosphorus and nearinfrared light. *Adv. Mater.* **2018**, *30*, 1801808.
[166] Shen, X. K.; Zhang, Y. Y.; Ma, P. P.; Sutrisno, L.; Luo, Z.; Hu, Y.; Yu, Y. L.; Tao, B. L.; Li, C. Q.; Cai, K. Y. Fabrication of magnesium/zinc-metal organic framework on titanium implants to inhibit bacterial infection and promote bone regeneration. *Biomaterials* **2019**, *212*, 1–16.
[167] Joubani, M. N.; Zanjanchi, M. A.; Sohrabnezhad, S. A novel Ag/Ag3PO4-IRMOF-1 nanocomposite for antibacterial application in the dark and under visible light irradiation. *Appl. Organomet. Chem.* **2020**, *34*, e5575.
[168] Tao, B. L.; Lin, C. C.; He, Y.; Yuan, Z.; Chen, M. W.; Xu, K.; Li, K.; Guo, A.; Cai, K. Y.; Chen, L. X. Osteoimmunomodulation mediating improved osteointegration by OGP-loaded cobalt-metal organic framework on titanium implants with antibacterial property. *Chem. Eng. J.* **2021**, *423*, 130176.
[169] Kim, Y. K.; Han, S. W.; Min, D. H. Graphene oxide sheath on Ag nanoparticle/graphene hybrid films as an antioxidative coating and enhancer of surface-enhanced Raman scattering. *ACS Appl. Mater. Interfaces* **2012**, *4*, 6545–6551.
[170] Khanna, P. K.; Singh, N.; Kulkarni, D.; Deshmukh, S.; Charan, S.; Adhyapak, P. V. Water based simple synthesis of re-dispersible silver nano-particles. *Mater. Lett.* **2007**, *61*, 3366–3370.
[171] Chen, S. Y.; Lu, J.; You, T. H.; Sun, D. P. Metal-organic frameworks for improving wound healing. *Coord. Chem. Rev.* **2021**, *439*, 213929.
[172] Mao, D.; Hu, F.; Kenry; Ji, S. L.; Wu, W. B.; Ding, D.; Kong, D. L.; Liu, B. Metal-organic-framework-assisted *in vivo* bacterial metabolic labeling and precise antibacterial therapy. *Adv. Mater.* **2018**, *30*, 1706831.
[173] Blissett, A. R.; Deng, B.; Wei, P.; Walsh, K. J.; Ollander, B.; Sifford, J.; Sauerbeck, A. D.; McComb, D. W.; McTigue, D. M.; Agarwal, G. Sub-cellular *in-situ* characterization of Ferritin(iron) in a rodent model of spinal cord injury. *Sci. Rep.* **2018**, *8*, 3567.
[174] Jambovane, S. R.; Nune, S. K.; Kelly, R. T.; McGrail, B. P.; Wang, Z. M.; Nandasiri, M. I.; Katipamula, S.; Trader, C.; Schaef, H. T. Continuous, one-pot synthesis and post-synthetic modification of nanoMOFs using droplet nanoreactors. *Sci. Rep.* **2016**, *6*, 36657.
[175] Wang, D. D.; Zhou, J. J.; Chen, R. H.; Shi, R. H.; Xia, G. L.; Zhou, S.; Liu, Z. B.; Zhang, N. Q.; Wang, H. B.; Guo, Z. et al. Magnetically guided delivery of DHA and Fe ions for enhanced cancer therapy based on pH-responsive degradation of DHA-loaded

Fe3O4@C@MIL-100(Fe) nanoparticles. *Biomaterials* **2016**, *107*, 88–101.

[176] Khatoon, Z.; McTiernan, C. D.; Suuronen, E. J.; Mah, T. F.; Alarcon, E. I. Bacterial biofilm formation on implantable devices and approaches to its treatment and prevention. *Heliyon* **2018**, *4*, e01067.

[177] Easun, T. L.; Moreau, F.; Yan, Y.; Yang, S. H.; Schröder, M. Structural and dynamic studies of substrate binding in porous metalorganic frameworks. *Chem. Soc. Rev.* **2017**, *46*, 239–274.

[178] Motoyama, S.; Makiura, R.; Sakata, O.; Kitagawa, H. Highly crystalline nanofilm by layering of porphyrin metal-organic framework sheets. *J. Am. Chem. Soc.* **2011**, *133*, 5640–5643.

[179] Cui, C. L.; Liu, Y. Y.; Xu, H. B.; Li, S. Z.; Zhang, W. N.; Cui, P.; Huo, F. W. Self-assembled metal-organic frameworks crystals for chemical vapor sensing. *Small* **2014**, *10*, 3672–3676.

[180] Mazloom-Jalali, A.; Shariatinia, Z.; Tamai, I. A.; Pakzad, S. R.; Malakootikhah, J. Fabrication of chitosan-polyethylene glycol nanocomposite films containing ZIF-8 nanoparticles for application as wound dressing materials. *Int. J. Biol. Macromol.* **2020**, *153*, 421–432.

[181] Duan, C.; Meng, J. R.; Wang, X. Q.; Meng, X.; Sun, X. L.; Xu, Y. J.; Zhao, W.; Ni, Y. H. Synthesis of novel cellulose-based antibacterial composites of Ag nanoparticles@metal-organic frameworks@carboxymethylated fibers. *Carbohydr. Polym.* **2018**, *193*, 82–88.

[182] Liu, J. Y.; Sonshine, D. A.; Shervani, S.; Hurt, R. H. Controlled release of biologically active silver from nanosilver surfaces. *ACS Nano* **2010**, *4*, 6903–6913.

[183] Liu, Z. G.; Wang, Y. L.; Zu, Y. G.; Fu, Y. J.; Li, N.; Guo, N.; Liu, R. S.; Zhang, Y. M. Synthesis of polyethylenimine (PEI) functionalized silver nanoparticles by a hydrothermal method and their antibacterial activity study. *Mater. Sci. Eng. C* **2014**, *42*, 31–37.

[184] Kim, J. S.; Kuk, E.; Yu, K. N.; Kim, J. H.; Park, S. J.; Lee, H. J.; Kim, S. H.; Park, Y. K.; Park, Y. H.; Hwang, C. Y. et al. Antimicrobial effects of silver nanoparticles. *Nanomed. :Nanotechnol. , Biol. Med.* **2007**, *3*, 95–101.

[185] Huang, Y.; Zhao, M. T.; Han, S. K.; Lai, Z. C.; Yang, J.; Tan, C. L.; Ma, Q. L.; Lu, Q. P.; Chen, J. Z.; Zhang, X. et al. Growth of Au nanoparticles on 2D metalloporphyrinic metal-organic framework nanosheets used as biomimetic catalysts for cascade reactions. *Adv. Mater.* **2017**, *29*, 1700102.

[186] Feng, G. N.; Huang, X. T.; Jiang, X. L.; Deng, T. W.; Li, Q. X.; Li, J. X.; Wu, Q. N.; Li, S. P.; Sun, X. Q.; Huang, Y. G. et al. The antibacterial effects of supermolecular nano-carriers by combination of silver and photodynamic therapy. *Front. Chem.* **2021**, *9*, 666408.

[187] Gunawan, C.; Teoh, W. Y.; Marquis, C. P.; Amal, R. Cytotoxic origin of copper(II) oxide nanoparticles: Comparative studies with micron-sized particles, leachate, and metal salts. *ACS Nano* **2011**, *5*, 7214–7225.

[188] Fang, F. C. Perspectives series: Host/pathogen interactions. Mechanisms of nitric oxide-related antimicrobial activity. *J. Clin. Invest.* **1997**, *99*, 2818–2825.

[189] Wheatley, P. S.; Butler, A. R.; Crane, M. S.; Fox, S.; Xiao, B.; Rossi, A. G.; Megson, I. L.; Morris, R. E. NO-releasing zeolites and their antithrombotic properties. *J. Am. Chem. Soc.* **2006**, *128*, 502–509.

[190] Fox, S.; Wilkinson, T. S.; Wheatley, P. S.; Xiao, B.; Morris, R. E.; Sutherland, A.; Simpson, A. J.; Barlow, P. G.; Butler, A. R.; Megson, I. L. et al. NO-loaded Zn2+-exchanged zeolite materials: A potential bifunctional anti-bacterial strategy. *Acta Biomater.* **2010**, *6*, 1515–1521.

[191] Pinto, M. L.; Rocha, J.; Gomes, J. R. B.; Pires, J. Slow release of NO by microporous titanosilicate ETS-4. *J. Am. Chem. Soc.* **2011**, *133*, 6396–6402.

[192] Cattaneo, D.; Warrender, S. J.; Duncan, M. J.; Kelsall, C. J.; Doherty, M. K.; Whitfield, P. D.; Megson, I. L.; Morris, R. E. Tuning the nitric oxide release from CPO-27 MOFs. *RSC Adv.* **2016**, *6*, 14059–14067.

[193] Taylor-Edinbyrd, K.; Li, T. P.; Kumar, R. Effect of chemical structure of S-nitrosothiols on nitric oxide release mediated by the copper sites of a metal organic framework based environment. *Phys. Chem. Chem. Phys.* **2017**, *19*, 11947–11959.

[194] Duncan, M. J.; Wheatley, P. S.; Coghill, E. M.; Vornholt, S. M.; Warrender, S. J.; Megson, I. L.; Morris, R. E. Antibacterial efficacy from NO-releasing MOF-polymer films. *Mater. Adv.* **2020**, *1*, 2509–2519.

[195] Luan, X. K.; Wang, H. Z.; Xiang, Z. H.; Ma, Z. F.; Zhao, J. R.; Feng, Y.; Shi, Q.; Yin, J. H. Biomimicking dual-responsive extracellular matrix restoring extracellular balance through the Na/K-ATPase pathway. *ACS Appl. Mater. Interfaces* **2019**, *11*, 21258–21267.

[196] Vatansever, F.; de Melo, W. C. M. A.; Avci, P.; Vecchio, D.; Sadasivam, M.; Gupta, A.; Chandran, R.; Karimi, M.; Parizotto, N. A.; Yin, R. et al. Antimicrobial strategies centered around reactive oxygen species-bactericidal antibiotics, photodynamic therapy, and beyond. *FEMS Microbiol. Rev.* **2013**, *37*, 955–989.

[197] Tao, Y.; Ju, E. G.; Ren, J. S.; Qu, X. G. Bifunctionalized mesoporous silica-supported gold nanoparticles: Intrinsic oxidase and peroxidase catalytic activities for antibacterial applications. *Adv. Mater.* **2015**, *27*, 1097–1104.

[198] Jiao, L.; Wang, Y.; Jiang, H. L.; Xu, Q. Metal-organic frameworks as platforms for catalytic applications. *Adv. Mater.* **2018**, *30*, 1703663.

[199] Nath, I.; Chakraborty, J.; Verpoort, F. Metal organic frameworks mimicking natural enzymes: A structural and functional analogy. *Chem. Soc. Rev.* **2016**, *45*, 4127–4170.

[200] Sun, H. J.; Gao, N.; Dong, K.; Ren, J. S.; Qu, X. G. Graphene quantum dots-band-aids used for wound disinfection. *ACS Nano* **2014**, *8*, 6202–6210.

[201] Gao, L. Z.; Giglio, K. M.; Nelson, J. L.; Sondermann, H.; Travis, A. J. Ferromagnetic nanoparticles with peroxidase-like activity enhance the cleavage of biological macromolecules for biofilm elimination. *Nanoscale* **2014**, *6*, 2588–2593.

[202] Natalio, F.; André, R.; Hartog, A. F.; Stoll, B.; Jochum, K. P.; Wever, R.; Tremel, W. Vanadium pentoxide nanoparticles mimic vanadium haloperoxidases and thwart biofilm formation. *Nat. Nanotechnol.* **2012**, *7*, 530–535.

[203] Gao, L. Z.; Zhuang, J.; Nie, L.; Zhang, J. B.; Zhang, Y.; Gu, N.; Wang, T. H.; Feng, J.; Yang, D. L.; Perrett, S. et al. Intrinsic peroxidase-like activity of ferromagnetic nanoparticles. *Nat. Nanotechnol.* **2007**, *2*, 577–583.

[204] Wei, H.; Wang, E. K. Nanomaterials with enzyme-like characteristics (nanozymes): Next-generation artificial enzymes. *Chem. Soc. Rev.* **2013**, *42*, 6060–6093.

[205] Zhang, J. Y.; Chen, Y. P.; Miller, K. P.; Ganewatta, M. S.; Bam, M.; Yan, Y.; Nagarkatti, M.; Decho, A. W.; Tang, C. B. Antimicrobial metallopolymers and their bioconjugates with conventional antibiotics against multidrug-resistant bacteria. *J. Am. Chem. Soc.* **2014**, *136*, 4873–4876.

[206] Wang, D. D.; Jana, D.; Zhao, Y. L. Metal-organic framework derived nanozymes in biomedicine. *Acc. Chem. Res.* **2020**, *53*, 1389–1400.

[207] Ali, A.; Ovais, M.; Zhou, H. G.; Rui, Y. K.; Chen, C. Y. Tailoring metal-organic frameworks-based nanozymes for bacterial theranostics. *Biomaterials* **2021**, *275*, 120951.

[208] Hu, W. C.; Younis, M. R.; Zhou, Y.; Wang, C.; Xia, X. H. *In situ* fabrication of ultrasmall gold nanoparticles/2D MOFs hybrid as nanozyme for antibacterial therapy. *Small* **2020**, *16*, 2000553.

[209] Zhang, P.; Sun, D. R.; Cho, A.; Weon, S.; Lee, S.; Lee, J.; Han, J. W.; Kim, D. P.; Choi, W. Modified carbon nitride nanozyme as bifunctional glucose oxidase-peroxidase for metal-free bioinspired cascade photocatalysis. *Nat. Commun.* **2019**, *10*, 940.

[210] Wang, J. N.; Bao, M. Y.; Wei, T. X.; Wang, Z. Y.; Dai, Z. H. Bimetallic metal-organic framework for enzyme immobilization by biomimetic mineralization: Constructing a mimic enzyme and simultaneously immobilizing natural enzymes. *Anal. Chim. Acta* **2020**, *1098*, 148–154.

[211] Xu, W. Q.; Jiao, L.; Yan, H. Y.; Wu, Y.; Chen, L. J.; Gu, W. L.; Du, D.; Lin, Y. H.; Zhu, C. Z. Glucose oxidase-integrated metalorganic framework hybrids as biomimetic cascade nanozymes

for ultrasensitive glucose biosensing. *ACS Appl. Mater. Interfaces* **2019**, *11*, 22096–22101.

[212] Xu, B. L.; Wang, H.; Wang, W. W.; Gao, L. Z.; Li, S. S.; Pan, X. T.; Wang, H. Y.; Yang, H. L.; Meng, X. Q.; Wu, Q. W. et al. A single-atom nanozyme for wound disinfection applications. *Angew. Chem. , Int. Ed.* **2019**, *58*, 4911–4916.

[213] Zhong, X.; Xia, H.; Huang, W. Q.; Li, Z. X.; Jiang, Y. B. Biomimetic metal-organic frameworks mediated hybrid multienzyme mimic for tandem catalysis. *Chem. Eng. J.* **2020**, *381*, 122758.

[214] Hu, D. F.; Li, H.; Wang, B. L.; Ye, Z.; Lei, W. X.; Jia, F.; Jin, Q.; Ren, K. F.; Ji, J. Surface-adaptive gold nanoparticles with effective adherence and enhanced photothermal ablation of methicillinresistant *Staphylococcus aureus* biofilm. *ACS Nano* **2017**, *11*, 9330–9339.

[215] Teng, W. S. Y.; Zhang, Z. J.; Wang, Y. K.; Ye, Y. X.; Yinwang, E.; Liu, A.; Zhou, X. Z.; Xu, J. X.; Zhou, C. W.; Sun, H. X. et al. Iodine immobilized metal-organic framework for NIR-triggered antibacterial therapy on orthopedic implants. *Small* **2021**, *17*, 2102315.

[216] Yang, Y. Q.; Huang, K.; Wang, M. Q.; Wang, Q. S.; Chang, H. S.; Liang, Y. K.; Wang, Q.; Zhao, J.; Tang, T. T.; Yang, S. B. Ubiquitination flow repressors: Enhancing wound healing of infectious diabetic ulcers through stabilization of polyubiquitinated hypoxia-inducible factor-1α by theranostic nitric oxide nanogenerators. *Adv. Mater.* **2021**, *33*, 2103593.

[217] Yu, Y.; Tan, L.; Li, Z. Y.; Liu, X. M.; Zheng, Y. F.; Feng, X. B.; Liang, Y. Q.; Cui, Z. D.; Zhu, S. L.; Wu, S. L. Single-atom catalysis for efficient sonodynamic therapy of methicillin-resistant *Staphylococcus aureus*-infected osteomyelitis. *ACS Nano* **2021**, *15*, 10628–10639.

[218] Chilakamarthi, U.; Giribabu, L. Photodynamic therapy: Past, present and future. *Chem. Rec.* **2017**, *17*, 775–802.

[219] Lu, K. D.; He, C. B.; Lin, W. B. Nanoscale metal-organic framework for highly effective photodynamic therapy of resistant head and neck cancer. *J. Am. Chem. Soc.* **2014**, *136*, 16712–16715.

[220] Ethirajan, M.; Chen, Y. H.; Joshi, P.; Pandey, R. K. The role of porphyrin chemistry in tumor imaging and photodynamic therapy. *Chem. Soc. Rev.* **2011**, *40*, 340–362.

[221] Guo, J.; Wan, Y.; Zhu, Y. F.; Zhao, M. T.; Tang, Z. Y. Advanced photocatalysts based on metal nanoparticle/metal-organic framework composites. *Nano Res.* **2021**, *14*, 2037–2052.

[222] Cheng, L.; Wang, C.; Feng, L. Z.; Yang, K.; Liu, Z. Functional nanomaterials for phototherapies of cancer. *Chem. Rev.* **2014**, *114*, 10869–10939.

[223] Agostinis, P.; Berg, K.; Cengel, K. A.; Foster, T. H.; Girotti, A. W.; Gollnick, S. O.; Hahn, S. M.; Hamblin, M. R.; Juzeniene, A.; Kessel, D. et al. Photodynamic therapy of cancer: An update. *CA Cancer J. Clin.* **2011**, *61*, 250–281.

[224] Castano, A. P.; Demidova, T. N.; Hamblin, M. R. Mechanisms in photodynamic therapy: Part one-photosensitizers, photochemistry and cellular localization. *Photodiagn. Photodyn. Ther.* **2004**, *1*, 279–293.

[225] Ge, J. C.; Lan, M. H.; Zhou, B. J.; Liu, W. M.; Guo, L.; Wang, H.; Jia, Q. Y.; Niu, G. L.; Huang, X.; Zhou, H. Y. et al. A graphene quantum dot photodynamic therapy agent with high singlet oxygen generation. *Nat. Commun.* **2014**, *5*, 4596.

[226] Tan, L.; Li, J.; Liu, X. M.; Cui, Z. D.; Yang, X. J.; Yeung, K. W. K.; Pan, H. B.; Zheng, Y. F.; Wang, X. B.; Wu, S. L. *In situ* disinfection through photoinspired radical oxygen species storage and thermal-triggered release from black phosphorous with strengthened chemical stability. *Small* **2018**, *14*, 1703197.

[227] Hong, L.; Liu, X. M.; Tan, L.; Cui, Z. D.; Yang, X. J.; Liang, Y. Q.; Li, Z. Y.; Zhu, S. L.; Zheng, Y. F; Yeung, K. W. K. et al. Rapid biofilm elimination on bone implants using near-infrared-activated inorganic semiconductor heterostructures. *Adv. Healthc. Mater.* **2019**, *8*, 1900835.

[228] Yang, X. Y.; Wang, D. Y.; Shi, Y. H.; Zou, J. H.; Zhao, Q. S.; Zhang, Q.; Huang, W.; Shao, J. J.; Xie, X. J.; Dong, X. C. Black phosphorus nanosheets immobilizing Ce6 for imaging-guided photothermal/photodynamic cancer therapy. *ACS Appl. Mater. Interfaces* **2018**, *10*, 12431–12440.

[229] Yin, Z. H.; Chen, D. P.; Zou, J. H.; Shao, J. J.; Tang, H.; Xu, H.; Si, W. L.; Dong, X. C. Tumor microenvironment responsive oxygenself-generating nanoplatform for dual-imaging guided photodynamic and photothermal therapy. *Chemistryselect* **2018**, *3*, 4366–4373.

[230] Li, L.; Chen, Y. S.; Chen, W. J.; Tan, Y.; Chen, H. Y.; Yin, J. Photodynamic therapy based on organic small molecular fluorescent dyes. *Chin. Chem. Lett.* **2019**, *30*, 1689–1703.

[231] Dai, X. M.; Zhao, Y.; Yu, Y. J.; Chen, X. L.; Wei, X. S.; Zhang, X. G.; Li, C. X. Single continuous near-infrared laser-triggered photodynamic and photothermal ablation of antibiotic-resistant bacteria using effective targeted copper sulfide nanoclusters. *ACS Appl. Mater. Interfaces* **2017**, *9*, 30470–30479.

[232] Liang, S.; Deng, X. R.; Chang, Y.; Sun, C. Q.; Shao, S.; Xie, Z. X.; Xiao, X.; Ma, P.; Zhang, H. Y.; Cheng, Z. Y. et al. Intelligent hollow Pt-CuS janus architecture for synergistic catalysis-enhanced sonodynamic and photothermal cancer therapy. *Nano Lett.* **2019**, *19*, 4134–4145.

[233] Huo, M. F.; Wang, L. Y.; Wang, Y. W.; Chen, Y.; Shi, J. L. Nanocatalytic tumor therapy by single-atom catalysts. *ACS Nano* **2019**, *13*, 2643–2653.

[234] Yumita, N.; Nishigaki, R.; Umemura, K.; Umemura, S. I. Hematoporphyrin as a sensitizer of cell-damaging effect of ultrasound. *Jpn. J. Cancer Res.* **1989**, *80*, 219–222.

[235] Wang, X. N.; Ip, M.; Leung, A. W.; Xu, C. S. Sonodynamic inactivation of methicillin-resistant *Staphylococcus aureus* in planktonic condition by curcumin under ultrasound sonication. *Ultrasonics* **2014**, *54*, 2109–2114.

[236] Wang, X. N. ; Ip, M. ; Leung, A. W. ; Yang, Z. R. ; Wang, P. ; Zhang, B. T. ; Ip, S. ; Xu, C. S. Sonodynamic action of curcumin on foodborne bacteria Bacillus cereus and *Escherichia coli*. *Ultrasonics* **2015**, *62*, 75–79.

[237] Nakonechny, F.; Nisnevitch, M.; Nitzan, Y.; Nisnevitch, M. Sonodynamic excitation of rose bengal for eradication of grampositive and gram-negative bacteria. *BioMed Res. Int.* **2013**, *2013*, 684930.

[238] Wang, X. N. ; Ip, M. ; Leung, A. W. ; Wang, P. ; Zhang, H. W. ; Hua, H. Y. ; Xu, C. S. Sonodynamic action of hypocrellin B on methicillin-resistant *Staphylococcus aureus*. *Ultrasonics* **2016**, *65*, 137–144.

[239] Xu, C. S. ; Dong, J. H. ; Ip, M. ; Wang, X. N. ; Leung, A. W. Sonodynamic action of chlorin e6 on *Staphylococcus aureus* and *Escherichia coli*. *Ultrasonics* **2016**, *64*, 54–57.

[240] Zhuang, D. S. ; Hou, C. Y. ; Bi, L. J. ; Han, J. L. ; Hao, Y. R. ; Cao, W. W. ; Zhou, Q. Sonodynamic effects of hematoporphyrin monomethyl ether on *Staphylococcus aureus in vitro*. *FEMS Microbiol. Lett.* **2014**, *361*, 174–180.

[241] Huo, M. F.; Wang, L. Y.; Chen, Y.; Shi, J. L. Tumor-selective catalytic nanomedicine by nanocatalyst delivery. *Nat. Commun.* **2017**, *8*, 357.

[242] Li, W. P.; Su, C. H.; Chang, Y. C.; Lin, Y. J.; Yeh, C. S. Ultrasoundinduced reactive oxygen species mediated therapy and imaging using a fenton reaction activable polymersome. *ACS Nano* **2016**, *10*, 2017–2027.